Spatial Temporal Relationship between Land Use Land CoverChange and Land Surface Temperature in Chitwan District,Nepal

尼泊尔奇旺地区土地利用覆被与地表温度的时空关系

Amrita Darjee[a], Ling Chen[a]
[a]School of Forestry, Beijing Forestry University, Beijing, China

ABSTRACT

Land use land cover change (LULCC) and land surface temperature (LST) are two important indicators of global environmental change that have significant impacts on both natural and humansystems. Urban growth coupled with a rising population is resulting in increased demand for naturalresources, causing land use changes into megacities. In the context of climate change, the world is striving to find an effective way to be "carbon neutral". By the end of 2021, 136 countries in the world have put forward their "carbon neutral" commitments, among which Nepal has advanced its "carbon neutral" date to 2045, which is a very challenging task. Therefore, it is particularly importantto study LULCC and its relationship with LST in Nepal in recent decades, so as to provide scientificand empirical basis for relevant construction departments to make corresponding plans.

The main aim of this research was to assess the LULCC and its impact on LST using remote sensingand GIS techniques for 2002, 2012 and 2022 in Chitwan District, Nepal, in order to understand LULCC and their influencing factors in the past 20 years, to rationally evaluate environmental changes in this area. Firstly, Landsat images covering the study area were downloaded from USGS Earth Explorer, and normalized difference vegetation index (NDVI), normalized difference water index (NDWI) and normalized difference built-up index (NDBI) were calculated based on the corresponding bands of the images. After image pre-processing, a supervised approach with a maximum likelihood classifier was employed for the classification and generation of LULC maps for the mentioned time periods. Seven land use classes were identified as barren land, built-up area,cropland, forest, grassland, shrub and water bodies.

The results showed that almost all the land cover components have changed (gains or losses) in thetime period. Change detection analyses showed that built-up areas increased, especially in the last 10 years. The built-up area increased from 152 km^2 to 412.48 km^2 in the total study area between2002 and 2022. The rate of urbanization was dramatic between 2012 and 2022. Cropland area decreased by 11.24%, grassland area decreased by 4.14%, and shrub area increased from 2.15% to 6.08% from 2002 to 2022. In terms of the forest area, it increased from 1393.51 km^2 to 1492.31 km^2 (2002-2012), later in 2022, the area decreased 67.54 km^2. It was observed that there has been arapid change from cropland to built-up areas. The LST also dramatically changed over the time period. The highest LST in the study area was observed in 2022 (40.96°C) and it increased by 5.3°Cfrom that of 2002 (35.66°C). Therefore, it is crucial to enhance the urban planning, including adopting green city technology, to mitigate the rising LST.

Nepal, as one of the least developed agricultural countries in the world, has been seriously affectedby urbanization in recent years. The area of vegetation in Chitwan (including cultivated land, grassland, shrub and forest) has been reduced to varying degrees, and the LST has also increased significantly, which needs to attract the attention of some concerned authorities. This study providesscientific support and empirical evidence for the concerned authorities to promptly act upon the issue and formulate plans accordingly.

Keywords: Land use land cover, Land Surface Temperature, Urbanization, Remote sensing

1. Introduction

The geologic record shows multiple periods of warming and cooling related to the earth's climate. But recently, anthropogenic factors have caused significant changes in the earth system, and as a result, the entire planet is through a rapid warming cycle that is linked to a number of effects, including sea level rise, glacial melt, and unpredictability of weather patterns. According to the fourth assessment report published by the Intergovernmental Panel on Climate Change (IPCC), the global surface temperature will rise by 1.1– 6.4℃ by the end of the century (Fischlin et.al., 2007). Land use change has impact nearly a third (i.e., 32%) of the world's geographical surface since 1960(Winkler et al., 2021). A wide range of environmental and landscape characteristics are impacted by changes in land use and land cover (LULC) including the quality of water, land, and air resources,ecosystem processes, and the climate system itself. The major reasons attributable for such changesinclude surface effect and greenhouse gases fluxes. Changes in LULC should be regularly monitoredsince they have a negative influence on the environment, particularly by warming urban microclimates (Heinal et al., 2015; Policelli et al., 2018). The pattern of LULC is also dependent onhumans' utilization of natural and socio-economic variable throughout the course of time and space. Land use and land cover change (LULCC) is an extremely complicated process that can assume various shapes and progress at varying rates and magnitudes. Depending on its scale, its dynamics will change (Keyser & Kaiser, 2010). Land use change is the manipulation of land cover by humansfor numerous purpose including food, fuel wood, forage, litter, medicine, raw materials and recreation. Land cover changes can occur even in the absence of human activities through natural processes. So LULCC is influenced by numerous socioeconomic, environmental and political factors (Ojima et al., 1994). To determine the causes of change, processes and effects of LULCC, ithas been examined from several perspectives.

The study of LULCC is crucial to understanding of global environment change. In order to strengthen concepts of land use patterns, urban intensity, urban diversification, urban heat phenomena, along with other factors, understanding LULC has become increasingly crucial. This

because it can help to understand aspects of urban dynamics such as geography, morphology, ecology, and sustainability. However, due of various driving forces, the dynamics of LULC changehave not been consistent around the world. Change in LULC has been influence by population pressure, human activities, and development (Haregeweyn et al., 2015; Meshesha et al., 2014). Geospatial data is pivotal to adapting to the current land use pattern, planning for anticipated futurechanges, and assessing their effects on infrastructure and the surrounding environment. The classification of LULC serves as a warning system, highlighting the advantage of environmental conservation initiatives like afforestation while alerting people actions that harm the environment. LULC analysis can detect the human activities and natural world. In developing nation like Nepal, unplanned urbanization is becoming a significant development issues and challenges.

Remote Sensing and GIS, which first appeared in early 1970s', are essential to the world especially for environmental scientist (Jayantha et. al., 2015). GIS and RS are effective tools for investigating urban dimensions, including LULC mapping, urban density, urban modeling, and environmental implications of urban development over time (Kumar et al., 2016). Remote Sensing provide fast, accurate and trustworthy information of earth surface at specific time intervals so, is a way that it is both efficient and affordable (Chen et al., 2017). Satellite images at various spatial, temporal, and spectral resolutions have proven most efficient role in monitoring LULC mapping (Aredehey,2018).The aspects of the LULCC dynamics are reliably measured over time using remotesensing data. Landsat satellite image analysis based on remote sensing has been acknowledge as aneffective and trustworthy technique for LULC analysis (Fu et. al., 2017; Tao et. al., 2015). Severalresearchers (Baumann et al., 2014; Butt et al., 2015; Chasmer et al., 2014; Churches et al., 2014; Dronova et al., 2015; Iqbal and Khan, 2014; Naqvi et al.,

2014, Zhang et al., 2013) has used remote sensing data to analyze land use classification and monitoring, managing land degradation and analyze land use change. Studies of environmental deterioration using remote sensing and GIS are more efficient in terms of cost, time and area coverage than field surveys.

LST is a key parameter to measure urban health with respect to LULCC (Govinda and Ramesh, 2018). As, a consequence of anthropogenic climate change it contributes to the warming and increased LST globally. LST is connected to the planetary boundary layers combined with

thermal condition and surface energy balance (Jin, 2004). A solution for the absence of ground- based temperature data is to calculate LST from thermal infrared remote sensing data (Geremeskeland Abera, 2017); Liu et al., 2018). The growth of urbanized area, has resulted in deforestation andincrease in the average global surface temperature rise is caused by the depletion of the ozone layerthis both might be directly contributing factor to the raise in LST. The connection between the landsurface and atmosphere involves numerous processes and feedback, all of which has the potential to change simultaneously. These interactions determine LST, which is a crucial component of the climate system (Cong and Brandy, 2012).

Although Nepal is a mountainous nation that makes up two-thirds of the Himalayan region (Rokayaet al., 2012), its primary economic activities are based on agriculture. Nepal is divided into five physiographic regions: Terai, the Siwalik range, Hill, Middle mountain and High mountain. Even with slight changes in the low land area of Terai, the Middle Mountain and High Mountain regionsare more susceptible to LULC and are more severely affected by it (Khanal, 2002). Due to the steepgradient of Nepal's mountain slopes, this type of impact is not just restricted to locations where change occurs, but also readily spreads with additional influence in the plains and low land areas. Since the 1970s, there have been several concerns with economic growth, human activities, and theenvironment generally in Nepal due to the rate of forest land degradation and expansion in farmland (Collins & Jenkins, 1996). The Himalayan Environmental Degradation theory (Ives & Messerli, 1990) claims that Nepal's LULC difficulties are directly related to mass forest degradation induced by economic activity based on natural resources, high population growth rates,and poverty.

Urban planning and administration now face new difficulties as a result of this rapid and uncontrolled urbanization. Hence, in order to build urban settlements and adapt to the changing environment, urban planners, policymakers, and citizens of cities must come up with new and inventive solutions (Hoelscher & Aijaz, 2016). The permanent loss of vegetation and an increase inbuilt-up areas are two of urbanization's main effects (Sharma et. al., 2013). This modifies the local climate, which has an impact on the urban environment's health.

The GIS and remote sensing techniques were applied in this research to detect the LULCC and LSTpattern and to analyze their relationship over Chitwan district during 2002, 2010 and 2022.

Research on the relationship between LST and LULC with topographic elements in the Terai regionhas not been done. Therefore, the research was conducted in order to assess map and evaluate the historical status and contemporary changes of LULC in Chitwan District as well as to identify the composition and distribution of main LULC categories. The research was meant to build a monitoring plan for operational usage. The research's findings were intended to provide important information to policy makers and resource managers regarding the areas where immediate deforestation mitigation measures were needed for sustainable management,

Research questions and objectives

The purpose of this study is to identify and analyze patterns of LULCC through time and its potential indications on LST in Chitwan District, Nepal. Also, to indicate the composition and distribution of major LULC

types using Landsat imagery. It helps to prioritize management, sustainable development, and conservation initiatives.

To achieve the general objective, four specific objectives were formulated as follows:

(1) To assess the LULCC in Chitwan based on the analysis of satellite imagery.

(2) To calculate the LST in the study area from 2002, 2012 and 2022.

(3) To determine LST change on each LULC type and investigate the relationship betweenLST and LULC characteristics.

(4) To examine the relationship between LST and satellite indices like NDVI, NDWI, NDBIfrom 2002 to 2022 in Chitwan District.

2. Study area and Data

2.1 Study Area

Chitwan district (27°36′21.60″N, longitude 84°22′47.28″ E) is one of the 77 districts of Nepalthat is located at the southwest corner of Bagmati Province. Chitwan covers an area of 2,238.39 km²i.e., 1.5% of the total area coverage of Nepal. The Makwanpur district in the east, the Parsa Districtand Bihar, India in the south, and the Nawalparasi District along the Narayani River in the west border the district. The Narayani River is the main river of Chitwan that separates the district's western boundary and flows from north to east. Siwalik region makes up the majority of the Chitwandistrict (86.5%), followed by the Mid-mountain region (12.7%) and Terai region (0.8%). The district's elevation ranges from 244 to 1945 meters. Administratively, the district is made up of seven municipalities, of which one is a metropolitan city, five are urban municipalities, and one is a ruralmunicipality. According to the 2021 national census, Chitwan had a population of 722,168 and a population density of 325.6/km². The population has increased by 2.1% annually since the 2011 census.

Tropical and subtropical forests are a distinctive feature of the Chitwan district. The district has a range of climatic seasons. Mainly Chitwan’s climate is characterized by a tropical monsoon and high humidity throughout the year. During the hottest days of the year, temperatures can occasionally rise as high as 29°C (84°F), with the average maximum temperature hovering around 27°C (80°F). The average minimum temperature in the colder months, like January, is 3°C (38°F). Chitwan receives an annual average rainfall of around 1900 mm minimum rainfall of 6mm in November and maximum rainfall of 645 mm in July. According to NAPA rankings for climate change vulnerability, the Chitwan district is classified as High Vulnerability, with a vulnerability index ranging from 0.061 to 0.786.

Situated at the base of the Himalayas, Chitwan harbors a remarkably diversified assortment of plantsand animals. Chitwan National Park located in the subtropical lowland of this district is Nepal’s firstNational park and a World Heritage Site that was established in 1973. Sal (Shorea Robusta) forest,a moist deciduous plant species native to the Terai region, makes up around 70% of the park'stotal natural vegetation. The other types of vegetation include grassland, riverine forest, and Sal (*Shorea Robusta*) with Chir pine (*Pinus Roxburghii*). The National Park host a greater biological diversity with over 55 amphibian and reptiles, 525 bird, and 50 mammal species in the park. It is

home to one of the remaining populations of single-horned Asiatic rhinoceroses and one of the

Bengal Tiger's last refuges. The Chitwan district is a prime location for conducting this study as this region has undergone several changes in its land use patterns throughout the years. In the 1950s,the district was partially deforested to make room for settlement, cultivation, and the eventual eradication of malaria (Zvoleff & An, 2014).

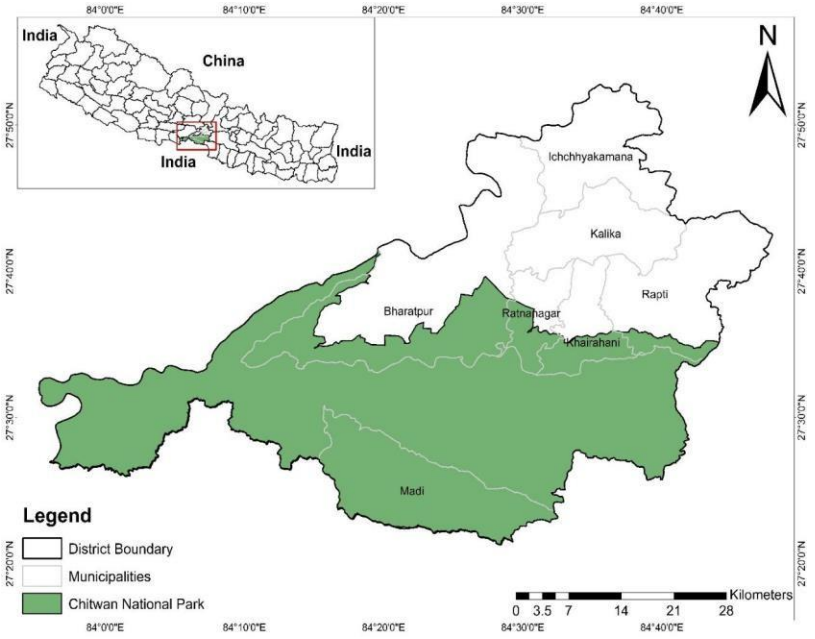

Figure 2: The geographic location of the study Area (Chitwan District)

Data collection

Primary data collection

(1) Data acquisition

For this study, two types of Landsat satellite images of past three decades 2002, 2012 and 2022 Landsat 7 Enhanced Thematic Mapper Plus (ETM+) and Landsat 8 Operational Land Imager (OLI)/Thermal Infrared Sensor (OLI/TIRS) Collection 2 Level 1 Science Products was retrieved from United States Geological Survey (USGS) (Source: https://earthexplorer.usgs. gov). There are two Landsat levels: Level-1 and Level-2. The image data in the Level-1 product is kept in Digital Numbers (DNs), which can then be translated to Top-of-atmosphere reflectance or at- sensor radiance using the product's supporting metadata. Level-2 products are the image data thathas been calculated using Level-1 products. Surface Reflectance and Surface Temperature scene- based products are included in level-2.

Landsat 8 image data files are comprised of 11 spectral bands with a spatial resolution of 15 meters

for the panchromatic band 8 and 30 meters for bands 1 to 7 and bands 9 to 11. Likewise, Landsat 7 ETM+ images are composed of eight spectral bands, with bands 1–7 having a spatial resolution of 30 meters and panchromatic band 8 having a resolution of 15 meters. The Level 2 Science Products however do not include a panchromatic band.

The cloud cover range was kept between 0-10% to avoid distortion of satellite images from clouds andcloud shadows. The distortion could potentially misrepresent land surface featuresand modify the reflectance of ground objects (Zhu & Helmer, 2018). As the percentage of cloud coverage was kept very low while downloading the Landsat product, there were very few satellite images available for applications. Therefore, satellite images were obtained for the month of October and November. Normally, early-season satellite images are suggested for satellite

time series construction as late- season images are susceptible to senescence and early snowfall (Wang et al., 2022). This study area, however, offers lowland climatic conditions and comprises low-latitude forests, so there are no snowfall records to date.

Table 1: Characteristics of Satellite Data used in Present Study

Year	Satellite	Sensor	Acquisition Date	Resolution Source
2002	Landsat 7	ETM+	02.04.2002 25.04.2002	30m United States Geological Survey (USGS) (https://earthexplorer.usgs.gov)
2012	Landsat 7	ETM+	15.05.2012 22.05.2012	30m United States Geological Survey (USGS) (https://earthexplorer.usgs.gov)
2022	Landsat 8	OLI	24.04.2022 25.04.2022	30m United States Geological Survey (USGS) (https://earthexplorer.usgs.gov)

(2) Topographic map

Besides Landsat images, the secondary data that was used in this research was high-resolution topographic maps. A topographical data layer was used to delineate administrative boundaries, contour, hydrology and other forms of LULC on the scale of (1:25,000). These data were obtained from the official records of the Survey Department of Nepal, ICIMOD. It was digitized manually. The obtained information helps in ground verification for supervised likelihood classification and accuracy assessment of classification of satellite image.

2.1.1 Secondary data collection

Secondary data and information were collected through review of relevant literature, Ministry of Forest and Soil Conservation, DOF, DSCWM, Division Forest Office, concerning NGO's and

INGO's such as Integrated Centre for Integrated Mountain Development (ICIMOD) and other agencies. Various web sites and documents through internet will also be studied during the secondary data collection.

3. Methodology

3.1 LULC Classification

Landsat satellite images from the Landsat 8 and Landsat 7 obtained in 2002, 2012 and 2022 were used for the classification procedure and study of the various LULC classes. Radiometric, Atmospheric and Sun angle corrections of respective Landsat imageries were carried out. LULC maps for change detection analysis were

generated using digital supervised classification with a maximum likelihood classifier (Lillesand et al. 2004) in Arc GIS 10.7. Supervised classification is when the user creates the spectral signatures of well-known classes, such as urban and forest, and the program then assigns each pixel in the image to the cover type to which its signature is most similar. This type of classification is most frequently utilized for quantitative assessments of remote-sensing image data.

Data sets were trained using the pixel color's tone. Polygons were drawn and placing them in an AOI (Area of Interest) layer allowed for the creation of training sites in the images. With the establishment of a specific area of interest (AOI), also known as training classes, the supervised categorization is used.

Table 2: LULCC classifications scheme

S. N.	LULC Classes	Description
1	Barren Land	The class comprises bare fields, rock-strewn surfaces, and other soil types that are perpetually devoid of plants.
2	Built-up Area	This class represents residential area, commercial buildings, roads and other manmade structures.
3	Cropland	Land devoted to the cultivation mainly rice, mustard; maize, and vegetables is included in this class.
4	Forest	This class corresponds dense trees and tall vegetation and also includes protected areas, national and private forest.
5	Grassland	This class includes, Generally open and continuous, fairly flat areas of grass.
6	Shrub	This class includes low-growing woody plants and other bushy plants that are primarily found along the edges of forests.
7	Water Bodies	Open water bodies such as rivers, reservoirs and lakes are included in this class

Polygons were merged and set up in the signature editor to train each individual class. These polygons were combined and assigned a unique class name. The signature file (.sig format) was thencreated from the signature editor file. In this research, three signature files for different year were created to train the 2002, 2012 and 2022 data sets. Finally, the supervised image classification process was conducted using the trained data sets. For each lesson, more than one training area wereutilized. The training locations was selected in accordance with the Google

Map, Google Earth, and Landsat images.

3.2 Accuracy Assessment

Accuracy assessment is one of the most crucial subsequent steps in the classification process.In this study, accuracy assessment w a s performed by comparing a map produced from remotely sensed data with another map obtained from some other source. Rapid changes in the landscape arecommon. Hence, it is ideal to get the ground reference as soon as the remote sensing data are acquired. Theobjective of accuracy assessment is to assess the precision with which the pixels were sampled into the appropriate land cover classes on a quantitative level. The accuracy of 2002,2012 and 2022 maps have been independently assessed. The main emphasis for accuracy assessment pixel selection that could be identified on both Landsat high-resolution images, GoogleEarth Pro and Google Map. The LULC data and map of ESRI, an American multinational GIS software company, is accurate and comparable and was used for this accuracy assessment too. Furthermore, historical records including topographical maps developed by the Survey Departmentof Nepal with scales of 1:25000 and 1:50000 was used for the assessment.

A number of quantitative methods were used for assessing image classification accuracy, includingoverall accuracy, user accuracy, producer accuracy, and Kappa statistics, which are one of the best quantitative procedures for image classification accuracy (Rahman et al., 2019). Kappa is a frequently cited measure of how effectively reference data and classified data agree however, the information it provides is constrained because it does not differentiate among quantification error and location error (Pontius, 2002). Classification errors may be caused by a variety of factors, suchas the topographic effect, a lack of samples for a particular class, misclassification of mixed pixels near class boundaries, or inaccurate ground control point locations that lead to errors in image-to- image registration Helmer et al., 2000 ; Foody, 2002).

Thus, accuracy assessment provides an overall accuracy of map as well as accuracy for each class in the map. The overall accuracy percentage was calculated by using following formula:

$$\text{Overall Accuracy} = \frac{\text{Total Number of Correctly Classified Pixels}}{\text{Total Number of Reference Pixels}} \times 100 \quad (1)$$

Along with overall accuracy, the accuracy of individual classes was also calculated for each class in each map. There were two methods used: user accuracy and producer accuracy. The percentage of correctly identified pixels to total reference pixels in each category is known as the producer's

accuracy. It accounts for the error of omission, which refers to the actual land cover type that was mistakenly left off the classified map. By dividing the total number of classified pixels in each category by the number of pixels that were correctly identified, the user's accuracy is determined (Pal and Ziaul, 2017).

The following formula is used to calculate the accuracy of the producer and the user:

$$\text{Producer Accuracy} = \frac{\text{Number of Correctly Classified Pixels in each Category}}{\text{Total Number of Reference Pixels in that Category}} \times 100 \quad (2)$$

$$\text{User Accuracy} = \frac{\text{Number of Correctly Classified Pixels in each Category}}{\text{Total Number of Classified Pixels in that Category}} \times 100 \quad (3)$$

A substitute measurement suggested by Verma et al. (2020) is the Kappa coefficient (K), which is utilized in addition to overall accuracy. Kappa coefficient (K) was calculated by dividing the total number of correctly classified pixels in the verification classes by the total number of pixels, and then subtracting the total number of ground verification pixels in each class (column total) timesthe total number of classified pixels in each class (row total) added together across all classes (sumof row total * column total) and dividing by the total number of ground verification pixels in each class (column total) times the total number of classified pixels (Pal and Ziaul, 2017; Choudhury et al. 2019). Kappa value lies between 0 and 1 (Hua and Ping, 2018). Kappa coefficient (K) is formally expressed as a percentage. The coefficient was calculated using following equation.

$$\text{Kappa Coefficient (K)} \frac{(TP \times TCP) - \sum(\text{Column Total} \times \text{Row Total})}{TP^2 - \sum(\text{Column Total} \times \text{Row Total})} \times 100 \quad (4)$$

Where, TP = Total Pixels, and TCP = Total Corrected Pixels.

3.3 Change detection of LULC

Information on land-cover and land-use change is useful for a variety of applications, such as deforestation, damage assessment, disaster monitoring, urban growth, planning, and land management. Altering the physical dimension of the spatial extent of the various LULC classes, LULCC affects many secondary processes that ultimately contribute to the degradation of the earth'secosystems. Change detection frameworks use multi-temporal datasets to qualitatively analyze thesechanges. For a deeper understanding of change mechanisms and for predicting the impact of change

on the environment and associated ecosystems at various scales, an inventory and monitoring of LULCC are essential (Chunghtai et al., 2021;Turner et al, 1995)

Change detection is a technique for analyzing site-specific multi-temporal imagery to look for short orlong term LULCC (Lillesand et al., 2004). A broad consensus exists in the literature regarding the definition of remote sensing for change detection. A broad consensus exists in the literature regardingthe definition of remote sensing for change detection. Change detection is a procedure used in GIS that analyzes how an area's features have changed over the course of at least two distinct periods. Comparing aerial photographs or satellite images of the area obtained at various dates is a common method of change detection. Change detection has been used extensively to evaluate shifting agriculture, deforestation, urban growth, and the effects ofnatural disasters like earthquakes and tsunamis, and use and land cover changes, among other things (Ramasubramanian, 2009). Singh 1989defines change detection as the process of detecting differences in a situation or with an object or feature at a location for different image atdifferent times. The four components of these definitions are method, place, images, and result. Each of these factors has its own potential effects on the results of change detection. In accordance to Lu et al., 2004, they are as follows:

a. The precision of geometric registration between multi-temporal images.
b. Adjusting multi-temporal images in perspective of other aspects
c. The quality of data;
d. Degree of complexity of landscape and environment in the study area;
e. Techniques or algorithms for change detection
f. Method for classification and change detection scheme
g. The analyst's degree of expertise
h. Knowledge of the research topic and study areas;
i. Funds and time availability

We performed the LULC change detection analysis after collecting the data, pre-processing it, supervised classifying it, assessing its accuracy, and assessing its change detection. Change detection statistics between the years 2002–2012, 2012–2020, and 2002–2022 have been created for this study. The percentage change was calculated by multiplying the observed differences by the total changes and dividing the result by 100 to determine the tendency of variation (Gajbhiye and Sharma, 2012). Mathematically,

Percentage Change = (Observed Change/ Sum of Change) *100 (5)

3.4 Calculation of normalized indexes

The high spatiotemporal resolution and near real-time observation capabilities of remote sensing make it a

highly effective tool for monitoring across vast areas (Wardlow et al. 2012).

To determine the relationship between LST and vegetation, Yue et al. (2007) and Wei et al. (2008)used the Greenness Vegetation Index (GVI), Soil Adjusted Vegetation Index (SAVI), Normalized Difference Vegetation Index (NDVI), Ratio Vegetation Index (RVI), and the Normalized Difference Built-up Index (NDBI). Different studies by Lawrence and Chase (2007);James and Charles (2014); Adeyeri and Okogbue (2014); Vlassova and Pe´rez-Cabello (2016) determined thatvegetation factors had a significant impact on the LST and energy balance of the areas under consideration.

3.4.1 Calculation of NDVI

The Normalized Difference Vegetation Index (NDVI), measures vegetation greenness and is helpful in determining vegetation density and evaluating alterations in plant health. The Normalized Difference Vegetation Index is derived from reflectance measurements in the near infrared (NIR) and red portions of the spectrum. It is the difference between NIR and visible red reflectance valuesadjusted over reflectance (Burgan and Hartford, 1993). Landsat 4-5 Thematic Mapper (TM), Landsat 7 Enhanced Thematic Mapper Plus (ETM+), and Landsat 8 Operational Land Imager (OLI)/Thermal Infrared Sensor (TIRS) Collection 1 and Collection 2 scenes which have been processed to Landsat Level-2 Surface Reflectance products are used to create the Normalized Difference Vegetation Index (NDVI) products. To calculate the Normalized Difference Vegetation Index, subtracting the red band from near infrared and then dividing to near infrared plus red band. NDVI is calculated by following equation.

$$\mathrm{NDVI}=\frac{(\mathrm{NIR}-\mathrm{RED})}{(\mathrm{NIR}+\mathrm{RED})} \tag{6}$$

Where, where RED and NIR stand for the spectral reflectance measurements acquired in the red (visible) and near-infrared regions, respectively. For Landsat 7 NIR is band 4 and RED is band 3 and for Landsat 8 NIR and RED is band 5 and band 4 respectively, which have been used to extractNDVI. Its value ranges from -1 to 1.

Generally, dense vegetation that may comprise a forest can be expected in a pixel if there is much more reflected near-infrared radiation than visible radiation. Stronger implications for healthy vegetation greenness are indicated by higher NDVI values (Jones and Vaughan, 2010). Further research has demonstrated a clear correlation between the NDVI and the ability of plant canopies tocapture energy. The negative values represent non-reflective surfaces like water, snow, clouds, and other non-vegetated areas, while the positive values represent reflectivesurfaces like a vegetated area(Burgan and Hartford, 1993). The temperature, moisture, and radiative characteristics of the earth's surface that determine LST have a direct relationship with vegetation (Weng, 2004).

The primary objective of applying NDVI is to enhance the processing of data about vegetation obtained through remote sensing. According to studies, NDVI is useful for identifying evergreen andseasonal forest types, savannah, dense vegetation, non-forest, and agricultural fields (Pettorelli et al.2005). It also helps to estimate various vegetation properties (Tian et al. 2017), biomass (Zhu and Liu 2015), chlorophyll content in foliage (Pastor-Guzman et al. 2015), plant yield (Vicente-Serranoet al. 2016), vegetation coverage (Dutrieux et al. 2015), and plant stress (Chavez et al. 2016). Theseestimates are frequently obtained by comparing ground-measured values of these variables with remotely sensed NDVI values. The resilience of NDVI-related models is directly correlated with NDVI related

models (Butt 2018).

3.4.2Calculation of NDWI

Remotely sensed data of vegetation and water from satellite is done using Normalized Difference Water Index (NDWI) (McFeeters, 1996). This kind of observation is employed mostly in the fieldsof agriculture and forest monitoring for evaluating the danger of fire, and it is especially appropriatein the context of environmental issues. NDWI is more sensitive to fluctuations in the water content of foliage in vegetation canopies than NDVI, yet it is less sensitive to changes in atmosphere (Gao, 1996; Wu et al., 2009).The NDWI is expressed as follows (McFeeters, 1996),

$$NDWI = \frac{(Green - NIR)}{(Green + NIR} \quad (7)$$

Where, Green is a green band such as Thematic mapper (TM) band 2, and NIR is a near infrared band such as TM 4. By utilizing green wavelengths, this index aims to increase water reflection, decrease the low NIR reflectance of water features, and enhance the high NIR reflectance of vegetation and soil features. Hence, although plant and soil typically have zero or negativevalues so they are suppressed, water features typically have positive values and are consequently boosted (McFeeters 1996). The lower values all the way to -1 are the telltale signals of drought

or non aqueous surface unless the area of intrest is the dry Surface and the higher values approaching +1 typically appear blue and correspond to either a high water content or surface.

3.4.3Calculation of NDBI

There are many indexes available for built-up area analysis. Normalized Difference Built-up Index(NDBI) is the most frequently used indices for analyzing built-up areas. Normalized Difference Built-up Index values lie between −1 and +1, low NDBI represent water bodies and larger positive NDBI values represent built-up or impervious concrete surfaces.

As suggested by Zhang (2006), to calculate NDBI, it was calculated by using following equation:

$$NDBI = \frac{(MIR - NIR)}{(MIR + NIR)} \quad (8)$$

Where NDBI is normalized difference built-up index, NIR is near infrared band 5 and MIR is middle infrared band 6 of Landsat 8 data. For Landsat 7 NIR Band 4 and MIR is Band 5. The derivedNormalized Difference Built-up Index values were further used to determine correlation coefficient

(r) between NDBI vs. LST and NDVI vs. NDBI and to give information to urban development planners to facilitate protection of urban environments.

3.5 Land surface temperature

3.5.1 LST related information

The effective radiating temperature of the earth's surface is controlled by a fundamental factor calledLST, which is a component of terrestrial thermal behavior (Kayet et al., 2016). It has a significant impact on hydrology, meteorology, and climatology and is a crucial component of both climateand biodiversity (Li et al., 2013). The World Meteorological Organization's Global Climate Observing System (GCOS) and NASA have both designated

it as one of the most significant earth system data records (EDR), a legacy national weather service (NWS) requirement, and an essential climate variable (ECV) (Tomlinson, 2011). Hulley (2019) says, The uses of LST have grown over time beyond its initial function as a climate change indicator. It serves as a crucial indicator for the energy redistribution at the land-atmosphere interface, soil moisture, plant water stress, drought monitoring, LULCC, urban heat island effects, heat stress, epidemiological investigations, and more. Furthermore, with the introduction of a new generation of hyperspectral sensors like the Infrared Atmospheric Sounding Interferometer (IASI) and Cross-Track Infrared

Sounder (CrIS), retrieval techniques have gone further than the typical thermal infrared andelectromagnetic waves (Tran et al., 2017). The estimation of LST from remotely sensed thermal infrared/operational land imager data has attracted much attention among the users (Hooker et al., 2018; Solanky et al., 2018). LST retrieval from regional, national and global remote sensed data offers unparalleled benefits and is considered one of the most popular techniques for researching theeffects of urban heat islands (Jiang & Lin, 2021). Geometrically corrected Landsat Thermal Infrared(TIR) band 6 and Landsat 8 Thermal Infrared (TIR) band 10 and 11 are used to calculate LST (Khin et al., 2012). Based on brightness temperature and the land surface emissivity, which is computed using the split window algorithm, one may derive the LST for a particular region (Rajeshwari and Mani, 2014, Md Shahid, 2014). The distinction between the surface equilibrium state and vigorous/vital for various applications is reflected by LST. LST is sometimes referred to as surface temperature monitoring using remote sensing and pixel-derived observations (Paramasivam, 2016). Urban LST characteristics are determined by the surface energy balance, which is controlled by factors like orientation, clouds and air, exposer to the sun, radiative abilityto reflect solar and infrared energy as well as ability to transmit infrared energy, availability of surface moisture to evaporate,and surface roughness (Voogt, 2000).

LULC is one of the main causes of the rise in LST, and several researchers conclude that uncontrolleduse of natural assets and land-use change are the main causes of the rise in LST. Oluseyi et al., 2011,studied that there are spatial linkages between alterations and the traits of specific land-use classifications or categories. At different latitudes, the impact of LULC shifts varies on LST, for instance in tropical temperate South Asia and East Asia (Shukla, 1990). The relationship between biodiversity, environmental degradation, and changes in land use in East Africa demonstrates that the region's original land cover was converted to grazing fields and residential areas (Matimal et al., 2009). As per Yue et al. (2007), the link between NDVI and LST is integrated by using Landsat7 ETM+ data in Shanghai. The outcome demonstrates that different LULC classes have verydiverse effects on the normalized differential vegetation index (NDVI) and LST determined by the Enhanced Thematic Mapper Plus sensor in the Shanghai urban environment. Due of their simplicity,physical basis, and operational capability, thermal sharpening models based on land-surface temperature and vegetation index (LST) have gained considerable attention. These models include the normalized difference vegetation index (NDVI). Normalize difference water index (NDWI), Normalized difference build-up index (NDBI) and fraction vegetation cover (FVC). Utilizing the DisTrad thermal sharpening model, Eswar et al., 2016 compare the relative performance of five

different VIs—NDVI, FVC, the normalized difference water index (NDWI), soil adjusted vegetation index (SAVI), and modified soil adjusted vegetation index (MSAVI), over natural as well as agricultural landscapes in India.

3.5.2 Process of LST Calculation

For Landsat 7

Conversion of DN to Radiance

$$L\lambda = (L_{MAX}\lambda - L_{MIN}\lambda)/ QCAL_{MAX} - QCAL_{MIN} \text{ x } (DN - QCAL_{MIN}) + L_{MIN}\lambda \quad (9)$$

Where,

Lλ = TOA spectral radiance (Watts/(m2 * srad * μm)Qcal = Quantized calibrated pixel value in DN

$L_{MAX}\lambda$ = maximum spectral radiance for the band $L_{MIN}\lambda$ = minimum spectral radiance for the band

$QCAL_{MAX}$ = maximum quantized calibrated pixel value (corresponding to $L_{MAX}\lambda$) in DN $QCAL_{MIN}$ = minimum quantized calibrated pixel value (corresponding to $L_{MIN}\lambda$) in DN DN is the pixel DN value

Convert Radiance into Top of Atmosphere BT (in Kelvin)

$$T = K2/ \ln (K1/ L\lambda + 1) \quad (10)$$

Where,

T = TOA brightness temperature in Kelvin,

Lλ = TOA spectral radiance (Watts/(m2 * srad * μm)K1 = Calibration constant 1

K2 = Calibration constant 2

Convert Degree Kelvin into Degree Celsius

The resulting temperature in the Kelvin scale will be converted to Celsius scale using thegiven equation,

$$C = T - 273.15 \quad (11)$$

Where T = Kelvin temperature and C = Celsius temperature.

The value 273.15°C is the absolute zero temperature for converting the Kelvin scale to the Celsiusscale.

(1) Calculation of TOA Spectral Radiance

In order to derive TOA spectral radiance from a Landsat satellite image, equation below wasused (USGS, 2016). OLI/TIRS data can be converted to spectral radiance using the radiance rescaling factors provided in the metadata file by using the given formula below:

$$L_\lambda = ML * Q_{cal} + AL \quad (12)$$

Where, L_λ is TOA spectral radiance (Watts/ (m^2* srad * μm); ML is Band-specific multiplicative rescaling factor from the metadata (RADIANCE_MULT_BAND_x, where x is the band number).Q_{cal} is Quantized and calibrated standard product pixel values (DN): Corresponds toband 10. AL is Band-specific additive rescaling factor from the metadata (RADIANCE_ADD_BAND_x, where x is the band number).

Conversion of TOA Spectral Radiance to Brightness Temperature

After obtaining TOA spectral reflectance radiance, brightness temperature was calculated accordingto equation below (Jim´enez-Munoz ˜ et al., 2014; USGS, 2016.The TOA Spectral Radiance data isthen converted to brightness temperature (BT) using the thermal constants(K1 AND K2) provided in the metadata file. According to Pal and Ziaul (2017), 0℃ is equivalent to

273.15 K, the units of BT is in Kelvin, hence it is necessary to convert the units to degree Celsius bysubtracting 273.15 from the calculated BT.

$$BT = (K2 / (\ln (K1 / L\lambda) + 1)) - 273.15 \quad (13)$$

Where, K1 is Band-specific thermal conversion constant from the metadata (K1_CONSTANT_BAND_x, where x is the thermal band number); K2 is Band-specific thermal conversion constant from the metadata (K2_CONSTANT_BAND_x, where x is the thermal band number).

Calculation of Proportion Vegetation (Pv)

The Carlson and Ripley (1997) equation was used to determine the Pv from the NDVI values obtained above. Fractional vegetation cover (FVC) is another word for vegetation cover. Pvvalues for areas with dense vegetation are 1, while Pv values for bare soil are 0. Therefore, Pv was determined from NDVI using the NDVI Threshold method.

$$Pv = (NDVI - NDVI_{min}) / (NDVI_{max} - NDVI_{min})^2 \quad (14)$$

Where,

Pv is proportion of vegetation; $NDVI_{min}$ is the minimum value of NDVI; $NDVI_{max}$ is maximum value of NDVI. The lowest and maximum values of an NDVI image are obtained from pixel value.

Calculation of Land Surface Emissivity (LSE)

The amount of radiance released by a black body at a given temperature and the percentage of radiance emitted by body temperature are referred to as the land surface emissivity (Zhao-Liang et al., 2013). As a result, the Pv layer provided the land surface emissivity, which was then utilized to calculate LST in equation.

$$\varepsilon = 0.004 * Pv + 0.986 \quad (15)$$

Where, ε is land surface emissivity; Pv is the proportion of vegetation.

Calculation of LST

Finally, Stathopoulou and Cartalis (2007) using the band 10 brightness temperature (BT) and land surface emissivity (ε) calculate the LST of the whole image following an equation. Using extraction by mask function in Arc Map 10.7 (Sun et al., 2012).

LST = BT/ 1+w*(BT/p)* ln (e) (16)

Where, BT is at-satellite brightness temperature; w is wavelength of emitted radiance (11.5um);p is h*c/s (1.438*10^-2mk). The value of p is 14380.

4. Results and Discussion

4.1 LULC and its accuracy assessment

4.1.1 LULC classes

In most cases, LULC classes are selected and fixed in accordance with the needs of a particular study or application. In this study, the study area has been categorized into seven LULC classes. The seven LULC classification used in this study are Barren land, Built-up area, Cropland, Forest, Grassland, Shrub and Water bodies. Table 2 above provides a thorough overview of these classes along with their distinctive characteristics.

From Figure 3, Figure 4 and Figure 5, we can conclude that the most of the cropland is converted into built-up

area over the time periods. Built-up area in 2002 and 2012 covered 7% of the area in Chitwan District. On the other hand, by 2022 the build-up area was increased by 11% as compared to 2002 and 2012 as shown in Table 3. Grassland was also decreased from 2002 to 2022 by 4%. Shrub area in 2002 was covered with 2%, but in 2012 its area decreased by 1% as compared to 2002 but after 2012 shrub area is increased and occupies with 6% of the total area by 2022. For the time being of the study period, Barren land has been decreased from 31.48 km2 to 17.81 km2 from 2002 to 2012 and 14.15km2 from 2012 to 2022. In addition waterbodies is also been decreased by

5.51 km2 in the study area by 2002 to 2022.

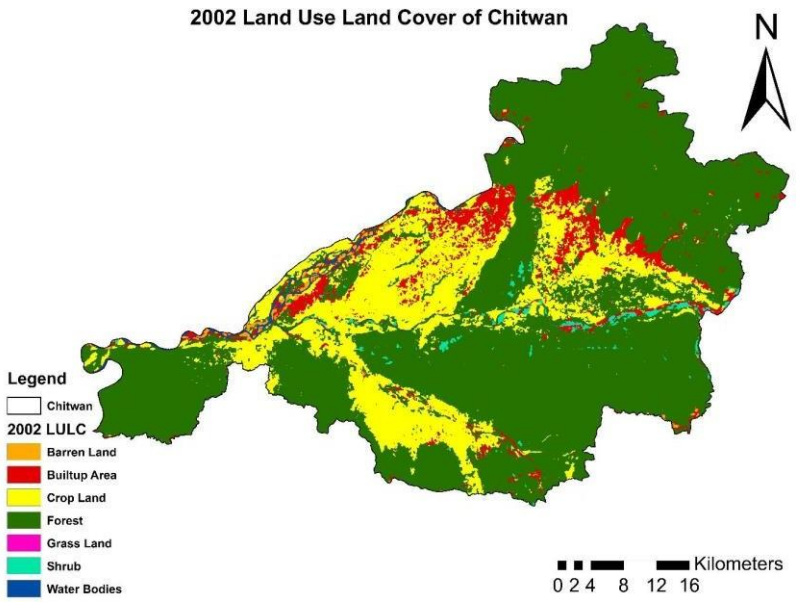

Figure 3: LULC map of year 2002 of Chitwan District

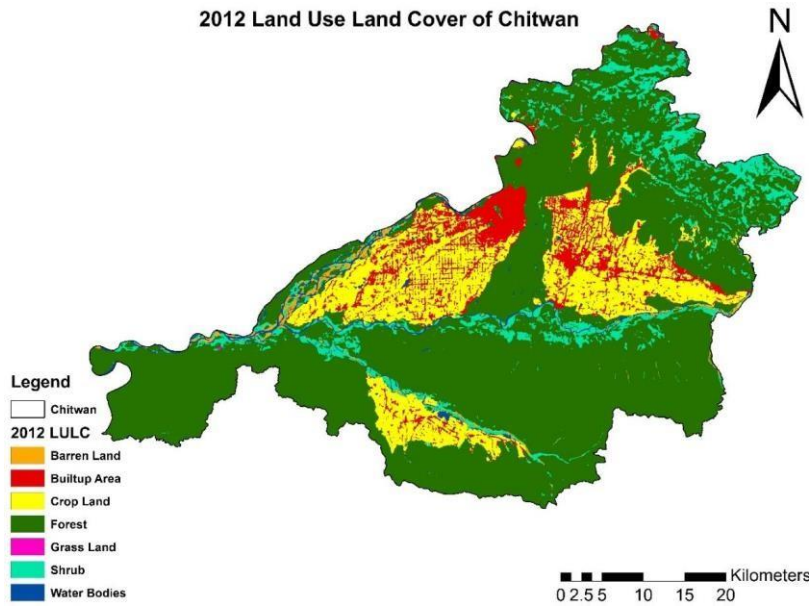

Figure 4: LULC map of year 2012 of Chitwan District

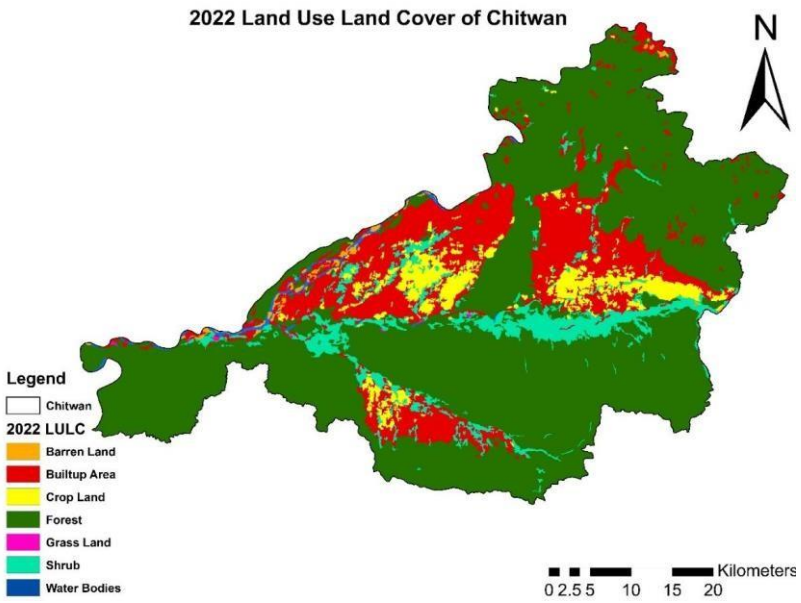

Figure 5: LULC map of year 2022 of Chitwan District

As given in table below (Table 3), in the year 2002, the forest area was 62% while cropland is coveredby 21%; the built-up area was covered by 7% while grassland covered about 5%, shrub land by 2%while Barren land and water bodies is followed by 1% each. In the year 2012, forest area was coveredby 67%, followed by cropland 16%, the built-up area was covered by 7% while the area was coveredby shrub is 6% and grassland is 2 % and area covered by barren land, water bodies is 1%,1% and 1% respectively. On the other hand, in the year 2022, forest area

occupy 64% of area, followed by 18% built-up area and 10% cropland; the shrub area was covered by 6% while the other classes like Barren land, grassland and waterbodies area coveran area of 1% each class. The area under the forest indicated the increasing trend from 2002 to 2012by 5% and from 2012 to 2022 it has decreased

by 3 % in the study area. Meanwhile, area of crop land is shrinking from 2002 to 2022 by 11%.

Table 3: The LULC area distribution of year 2002, 2012 and 2022 of Chitwan District

LULC classes	2002 Area (Km^2)	%	2012 Area(km^2)	%	2022 Area (km^2)	%
Barren Land	31.48	1%	18.31	1%	13.57	1%
Built-up Area	152	7%	165.48	7%	412.48	18%
Crop Land	475.29	21%	360.5	16%	223.73	10%
Forest	1393.51	62%	1492.31	67%	1424.77	64%
Grass Land	107.73	5%	40.38	2%	15.01	1%
Shrub	48.15	2%	136.19	6%	127.12	6%
Water Bodies	30.23	1%	25.22	1%	21.71	1%
Total	2238.39	100 %	2238.39	100%	2238.39	100%

Analyzing LULC allows for the examination of landscape patterns and features, which are crucial for comprehending the structure and conditions of lands as well as the dimension of ecological systems (Zhu et al., 2021). Understanding the extent of LULC is of the utmost importance sinceit is a key contributor to environmental changes such as biodiversity loss, habitat destruction, soil depletion, landslides, flooding, global climate change, and the impact of invasive and alien plant species (Wu, 2019; Chamnling & Bera, 2020).

4.1.2 Accuracy assessment

Classification accuracy is often impacted by the lack of fine details in the input. When images are used, the resolution of the image can affect the overall accuracy due to the need for generalizations. As a result, errors are always expected. In order to maintain accuracy, it is importantto use high resolution images and pay attention to the subtleties and nuances of the input. With a focus on the details, it is possible to increase the accuracy of the classification. For ensuring the effective use of land cover maps the inaccuracies must be quantitatively justified to go with statisticsproduced from remote sensing analyses (Sherefa, 2006).

Table 4: Accuracy assessment of LULC classification of 2002 using error matrix

LULC Classes	Forest	Cropland	Water	Built-up	Shrub	Barren Land	Grassland	Total	User Accuracy %
Forest	**38**	0	0	0	1	1	1	41	92.68
Cropland	0	**32**	0	4	1	0	0	37	86.49
Water	1	0	**33**	0	1	2	1	38	86.84
Built up	0	3	0	**36**	0	0	0	39	92.31

Shrub	2	1	1	0	**32**	2	1	38	84.21
Barren Land	2	1	1	1	0	**28**	0	33	84.84
Grassland	1	0	0	0	2	1	**22**	27	81.48
Total	44	37	35	41	37	34	25	Overall Accuracy	Cohen's Kappa
Producer Accuracy %	86.36	86.49	94.29	87.8	86.49	82.35	88	87.35%	0.85

Table 5: Accuracy assessment

of LULC classification of 2012 using error matrix

LULC Classes	Forest	Cropland	Water	Builtup	Shrub	Barren Land	Grassland	Total	User Accuracy%
Forest	**34**	0	0	2	1	38	89.47		
Cropland	1	**28**	0	3	0	1	33	84.75	
Water	0	**27**	0	0	1	31	87.1		
Built up	0	0	**24**	1	0	29	82.75		
Shrub	1	0	0	**32**	1	36	88.89		
Barren Land	0	2	2	0	**27**	0	32	84.38	
Grassland	1	1	0	1	**26**	29	89.66		
Total	37	35	30	31	36	31	30	Overall Accuracy	Cohen's Kappa
Producer Accuracy	91.89 %	80	90	90.32	88.89	87.1	86.67	86.84%	0.84

Table 6: Accuracy assessment of LULC classification of 2022 using error matrix

LULC Classes	Forest	Cropland	Water	Built up Area	Shrub	Barren Land	Grassland	Total	User Accuracy%
Forest	**42**	0	0	0	2	1	1	44	95.45
Cropland	0	**35**	0	5	1	1	0	37	94.6
Water	0	0	**36**	0	0	2	1	39	97.44
Built up Area	0	3	0	**27**	0	0	0	32	90.63
Shrub	2	2	0	0	**34**	0	1	36	91.67
Barren Land	1	0	3	1	0	**28**	1	32	93.75
Grassland	1	1	1	0	1	0	**27**	25	92
Total	46	41	40	33	38	34	31	Overall Accuracy	Cohen's Kappa
Producer Accuracy%	91.3	85.37	90	81.81	89.47	82.35	87.1	87.45%	0.85

An error matrix is the most standard and widely used technique by researchers to evaluate classification accuracy (Congalton et al., 1999; Sherefa 2006). For this specific study, various accuracy measures including overall accuracy, user accuracy, producer accuracy and Kohen's Kappa Coefficient are calculated. While user accuracy and producer accuracy identify the correctness of each individual classification, overall accuracy shows the accuracy of the entire LULC classification (Russell and Congalton, 2013). The likelihood of agreement in a categorized data set is indicated by the Cohen's kappa coefficient (Fleiss et al., 1969).

The classification techniques and methods of acquiring images usually result in some errors in landcover maps (Ogunjobi et al., 2018). For each of the 2002, 2012 and 2022 post classified images, theaccuracy evaluation tool of the supervised classifier randomly produced 253, 228 and 263 reference points using stratified random sampling was taken. Three error matrix tables for the year 2002, 2012 and 2022 are created in this study for the final LULC classification. The LULC classification shows an overall accuracy of 87.35%, 86.84% and 85.32% during 2002, 2012 and 2022, respectively, which are above the usual benchmark of 85% (Eniolorunda et al. 2016). User's accuracy and producer's accuracy are obtained from error matrix table of 2002, 2012 and 2022 as shown in Table 4, Table 5 and Table 6 below. During 2002, 2012 and 2022, the Cohen's Kappa

coefficient shows 0.85, 0.84 and 0.85 respectively.

4.2 LULC Change Detection from 2002 to 2022

Various LULC change detection studies take into account two clearly separated years for this procedure. The LULCC was analyzed and detected from the Landsat images at 10 years interval since 2002 to 2022. The change detection analysis presented in this paper is based on the statistics extracted from the classified land use and land cover maps of the Chitwan District of the year 2002 to2012, 2012 to 2022 and 2002 to 2022. Various LULC change detection studies take into account twoclearly separated years for this procedure.

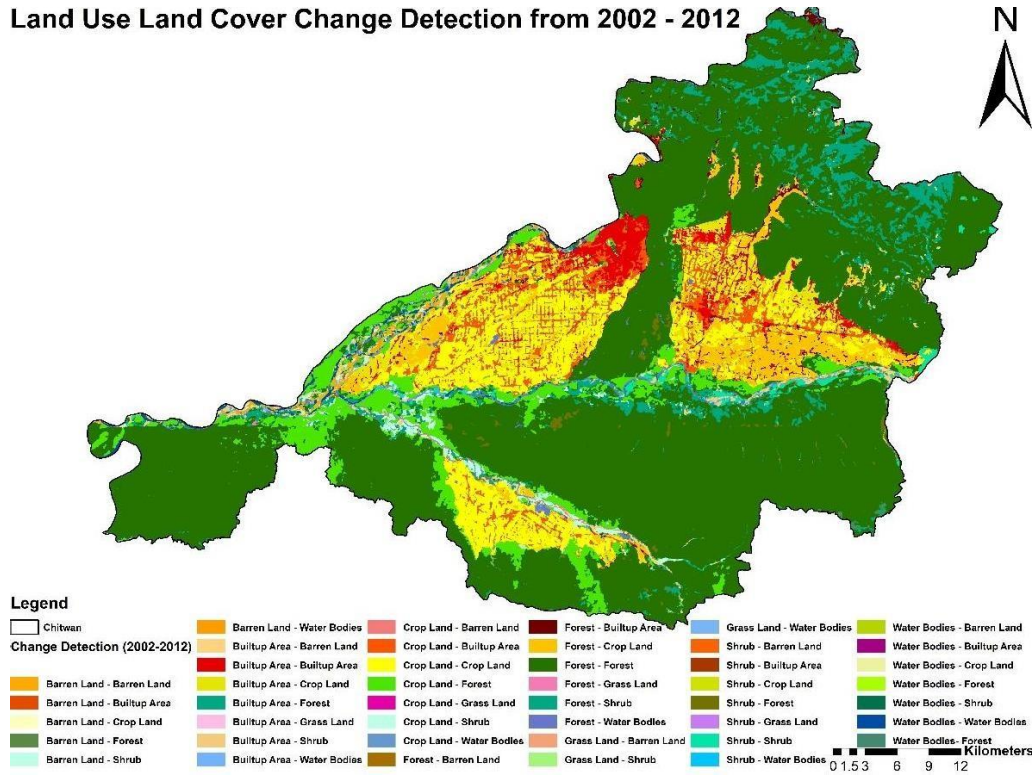

Figure 6: LULC change map of year 2002-2022 of Chitwan District

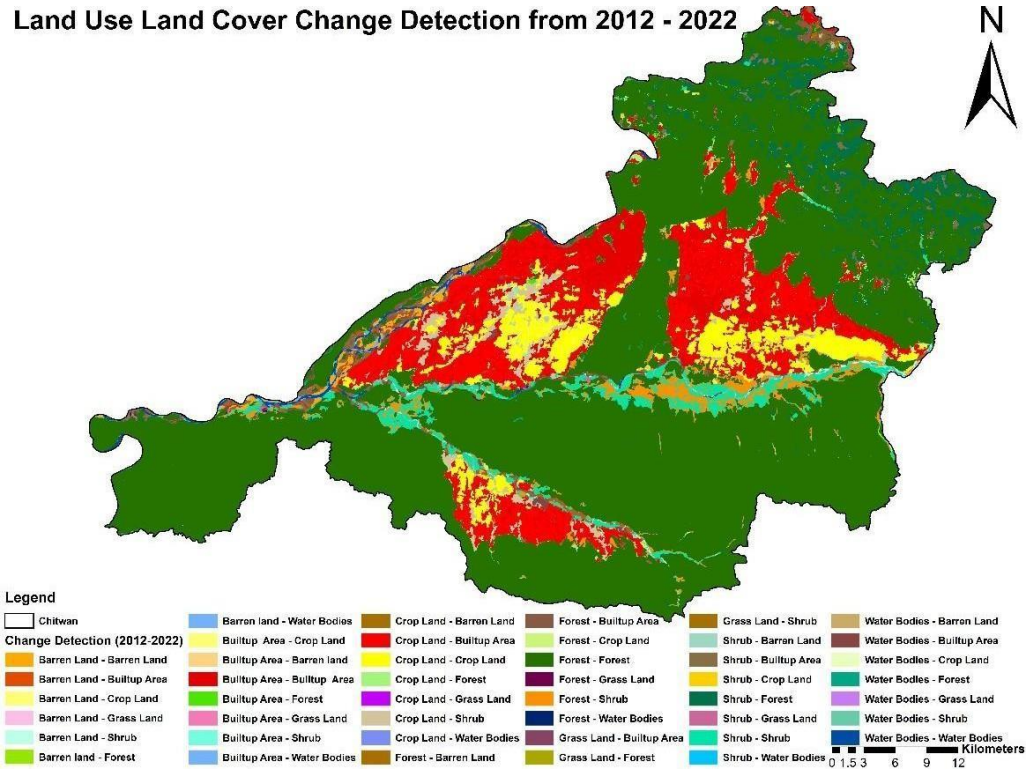

Figure 7: LULC Change map of year 2012-2022 of Chitwan District

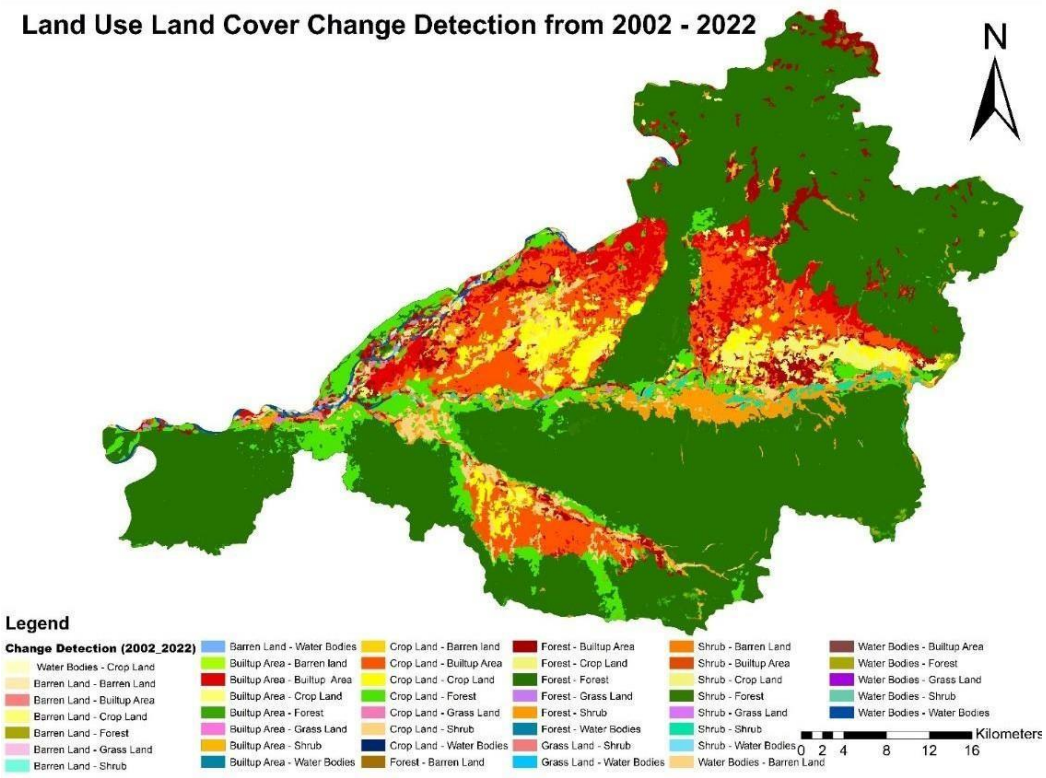

Figure 8: LULC Change map of year 2002-2022 of Chitwan District

Figure 8: LULC Change map of year 2002-2022 of Chitwan District

Table 7: Magnitude and Percentage of LULC change from 2002-2012,2012-2022 and 2002- 2022

LULC Classes	Area and Percentage						Magnitude of Change					
	2002		2012		2022		2002-2012		2012-2022		2002-2022	
	Area (km²)	Percent	Area (km²)	Percent	Area (km²)	Percent	Area (km²)	Percent	Area (km²)	Percent	Area (km²)	Percent
Barren	31.48	1.41	18.31	0.82	13.57	0.61	-13.17	-0.59	-4.74	-0.21	-17.91	-0.8
Builtup Area	152	6.79	165.48	7.39	412.48	18.43	13.48	0.6	247	11.03	260.48	11.64
Crop Land	475.29	21.23	360.5	16.11	223.73	10	-114.79	-5.13	-136.77	-6.11	-251.56	-11.24
Forest	1393.51	62.26	1492.31	66.67	1424.77	63.65	98.8	4.41	-67.54	-3.02	31.26	1.4
Grass Land	107.73	4.81	40.38	1.8	15.01	0.67	-67.35	-3.01	-25.37	-1.13	-92.72	-4.14
Shrub	48.15	2.15	136.19	6.08	127.12	5.68	88.04	3.93	-9.07	-0.41	78.97	3.53
Water Bodies	30.23	1.35	25.22	1.13	21.71	0.97	-5.01	-0.22	-3.51	-0.16	-8.52	-0.38

The results of the LULCC show that there is a significant change in LULC of the region from 2002 to2022 (Figure 6, Figure 7 and Figure 8).In the last two decades, the built-up area had the most

influence on the LULC change in the study area. A steady increment of the built-up area occurred each decade, with the highest increment of 11.03% observed from 2012 to 2022. Cropland was observed to be in continuous declining trend -11.24% decrease observed in 2002–2022. Forest was ina increasing trend between 2002 and 2012 but later it declined by -0.32% in the last decade. Within the period of 2002–2022, the built-up area was significantly increased by 11.64%. In the same period,barren land, cropland, grassland and waterbodies were decreased by -0.80%, -11.24% and -0.38%, respectively.

LULC changes occurred almost in the whole study area, except for the most part of Chitwan National Park and the northeast areas. In the Chitwan district, the percentage of forest cover didn't change consistently over time; instead, there were irregular fluctuations. From 2002 to 2012, there was a continual increment in the amount of forest cover, which was thereafter gradually reduced until 2022. In a similar study conducted by Stapp et al., 2015, it was found that between 1989 and 2005, the overall forest cover in all VDCs in the bufferzone of CNP decreased by 9.9%, and it thenincreased by 7.5% between 2005 and 2013; the net loss from 1989 to 2013 was 3.1%. Furthermore,Panta et al., 2008 found 7.95% decrement of forest coverage from 1981 to 2001 in the district.

In Nepal, community-based forest management approach has received widespread recognitionas the most effective method for fostering participatory forest governance and management. This initiative in Nepal is a part of a global movement toward forest decentralization that began four decades ago and offers local communities the capacity to manage and utilize forest resources legally. The country's forest cover increased from 26% to 45% between 1992 and 2016. Even though the district is adopting a community-based approach to forest management, there are still a number of factors that can be attributed for the reduction in Chitwan's forest cover. The Siwaliks zone, which includes the lowlands of Chitwan district, frequently engages in the repeated and unsustainable harvesting of non-wood forest products. This practice includes cutting down trees and saplings for timber and poles (often illegally) as well as collecting firewood for domestic use and sale (WWF, 2013).

In terms of built-up area, due to the growing population, this land use class has increased rapidly by11.64% in the Chitwan district in 2022. Various variables, however, are to blame for the rise in Chitwan’s urban area. The study region is located near the geographical center of Nepal in the eastern bank of the Narayani River, rendering it a financially viable zone. In a study in the western Terai conducted by Rimal et al.,(2020) it was discovered that from 1989 to 2016, more

agricultural lands were converted to urban lands in Chitwan. A key factor contributing to abrupt and severe changes in the built-up over the years is the growing population pressure brought on by migration and settlement. From 472,048 to 719,859, the population of the Chitwan district has nearlydoubled since 2001 (National Statistics Office, 2023). People typically migrate from the Hill to the Terai region because of food shortages, prospects, difficult lifestyles, poverty, and terrible climatic and relief circumstances. In Nepal's mid-hills, about one-third of the agricultural land has already been abandoned, and many people have moved into urban and semi-urban regions of Terai (Gazzardet al., 2016). Even the whole population of the hill and mountain regions (46%)is lesser than that of the Terai (54%).

The another land use class that experienced substantial change is crop land/agricultural land. The substantial loss of agricultural land is may be as a result of land degradation, such as erosion, whichis the movement of soil components by wind or water. Land loss in agriculture dates back to the 20th century. Even during the 1950s, significant amounts of farmland were destroyed in Chitwandistrict, that led to an increase in food shortages, poverty, and landlessness (Agergaard, 1999). Agricultural land abandonment has possessed the greatest threat to food

security and agriculture (Paudel et al., 2016). Rural regions of Chitwan, which had significant agriculturalland coverage,has already been transformed into peri-urban and urban areas as a result of the rapid urban population growth, and this trend is still going unabated (Timilsina et al., 2019).

The increase in shrub land in Chitwan district in 20 years provides multiple indications. Shrub landbeing regarded as an eventual consequence of deforestation and degradation (Adeyemi & Olowo, 2022). On the other hand, shrublands being those that resulted from human land use conversions ofprevious natural vegetation types (Goldstein & DellaSala). In addition to altering energy fluxes, regional climate, soil-atmosphere exchange of water, carbon, and nutrients, and ecological interactions between species, a significant increase in shrub cover modifies the organization of ecosystems (Myers-Smith et al., 2011). The rest of the land use classes in the Chitwan has stable change.

4.3 Changes of normalized indices

4.3.1 NDVI Changes

NDVI enhances vegetation and tends to be positive whereas water body features have negative values, and soil may have zero values nearby. Only red band and NIR band of Landsat images

are used for NDVI analysis. The NDVI model derived through Landsat images of 2002, 2012, and 2022 as shown in Figure 9, Figure 10 and Figure 11. Arc GIS 10.7 software was used to identify vegetation cover. In 2002, NDVI values ranges from −0.45098 to 0.758865; NDVI values during 2012, it ranges from −0.195636 to 0.578857, whereas for NDVI values of year 2022 ranges from -0.0918861 to 0.497717, which means the vegetation cover, has decreased in 2022 when compared to 2002 in Chitwan District. Higher NDVI indicated that places with the most vegetation and forest tended to be the most productive areas. Lower NDVI values, on the other hand, indicated that there are less productive places, such as bare soil, waterbodies, and built-up areas. As a result, the research area's most prolific and productive area exhibited a significant decline on the NDVI map. The study results revealed that high vegetative areas show low LST and vice versa in the studyarea over the study period.

Monitoring the dynamics of vegetation coverage is essential for determining the status of overall vegetation and creating strategies for long-term forest management. The NDVI value of Chitwan district has gradually decreased over the years. As per the results, Chitwan had dense green vegetationin 2002 but the vegetation gradually became sparse till 2022. According to a study of vegetation density using the NDVI in the Chitwan National Park from 1978 to 1999, it was found that the highlyvegetated area was reduced by 5.03 km2 in less than 10 years (Baidya et al., 2009). In contrast, Dai et al., 2021 studied the green vegetation dynamics of community forests in Chitwan from 1988 to 2018 and discovered that all forests have been steadily becoming greener since their establishment, with the average green vegetation cover of all forests rising from around 30% in 1988 to above 70% in 2018. The authors credited this improvement in the forest coverage to the successful implementation of community-based forest management. This might be due to NDVI being susceptible to changes in the atmosphere, including clouds, haze, and aerosols, which can impact thereflectance of light in the visible and near-infrared (NIR) wavelengths. It might be challenging to correctly interpret NDVI images because of mistakes in NDVI values.

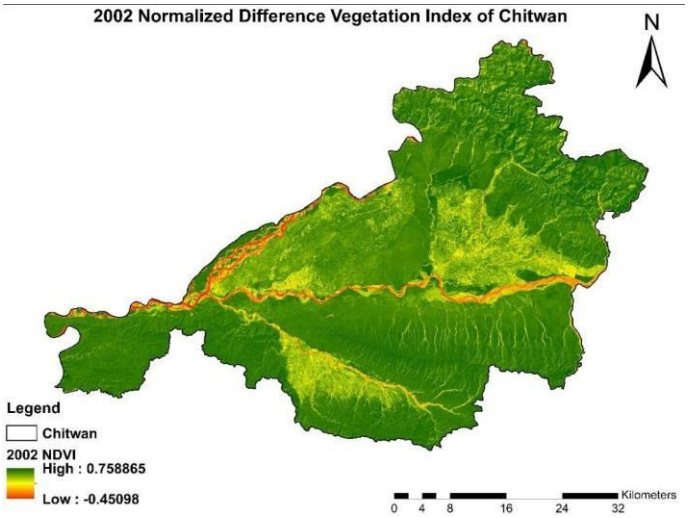

Figure 9: NDVI map of year 2002 of Chitwan District

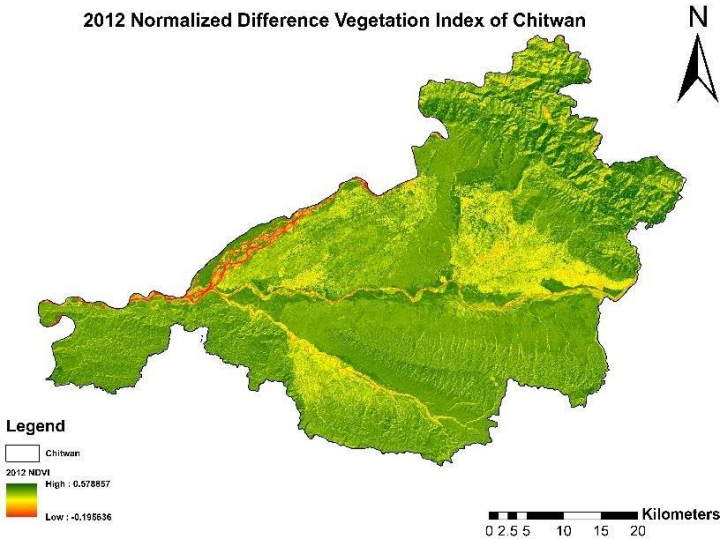

Figure 10: NDVI map of year 2012 of Chitwan District

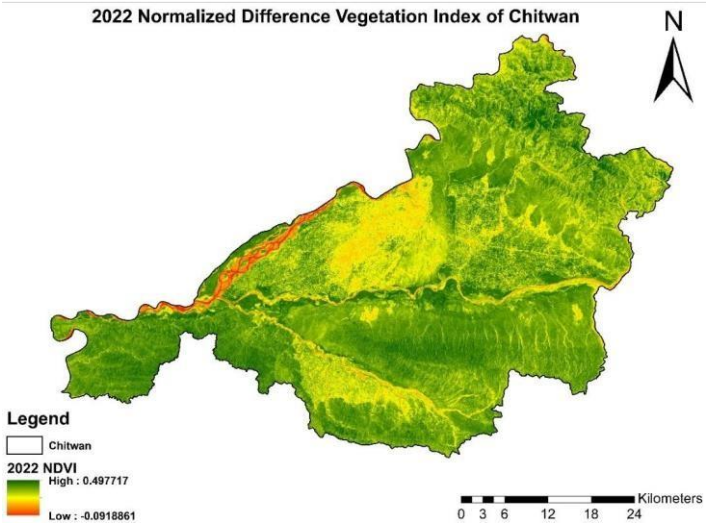

Figure 11: NDVI map of year 2022 of Chitwan District

4.3.2 NDWI Changes

The NDWI is identified to monitor the presence of water bodies. An index value of +1 indicatesa higher water content, and a value of -1 indicates an impervious area. There are scatter distribution of small to medium sizes of water bodies in Chitwan district. The spatial distribution of NDWI for 2002, 2012 and 2022 is shown in figures (Figure 12, Figure 13 and Figure 14). There are the changes in NDWI value during the study period. The resultant minimum and maximum NDWI values ranged from -0.505247 to 0.191314, -0.497736 to 0.147499 and - 0.442932 to 0.117893 on 2002,2012 and 2022 respectively in the study area. The study results show a decrement in positive NDWI values in 2022, indicating water bodies' shrinkage due to various reasons. It is noteworthy that the NDWI was decreased from 2002 to 2022.

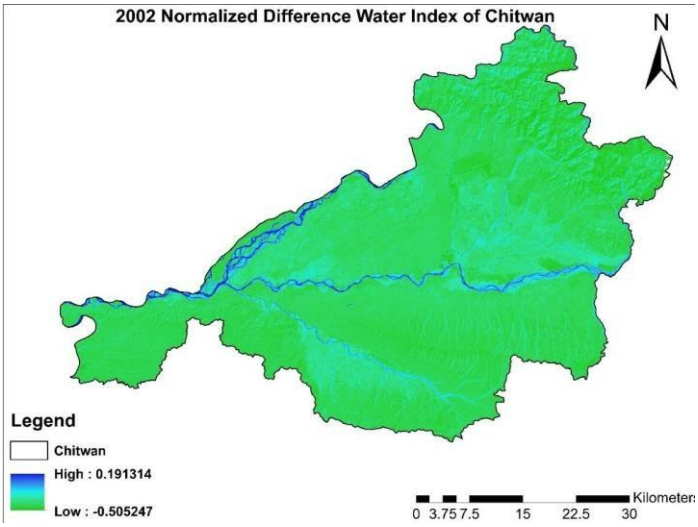

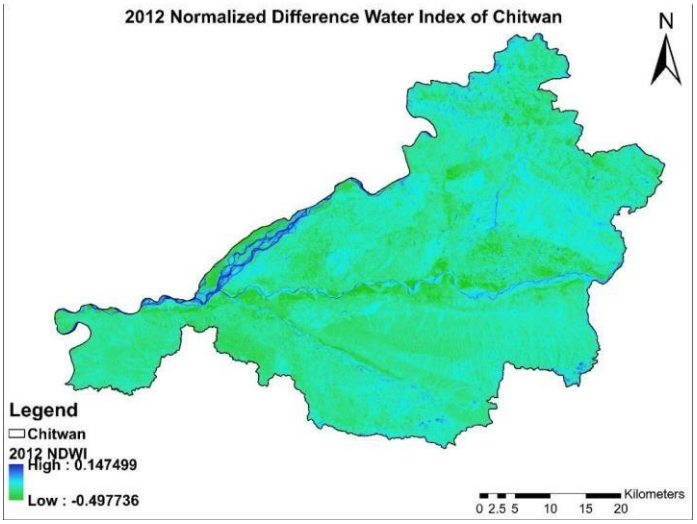

Figure 12: NDWI map of year 2002 of Chitwan District

Figure 13: NDWI map of year 2012 of Chitwan District

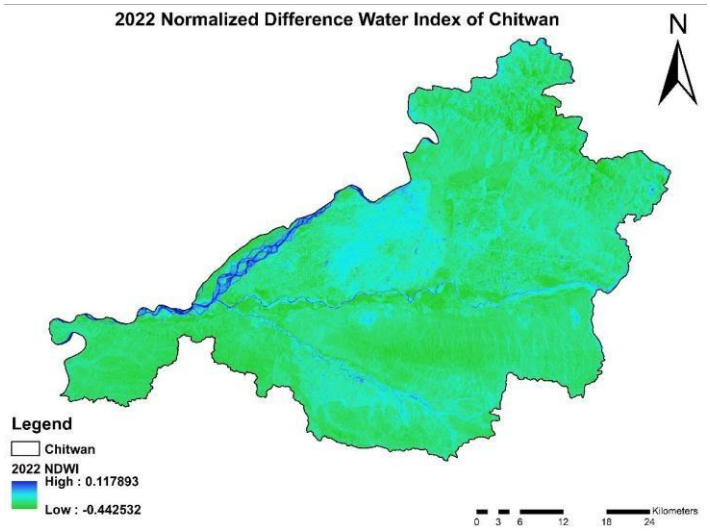

Figure 14: NDWI map of year 2022 of Chitwan District

4.3.3 NDBI Changes

The minimum and maximum NDBI values of the year 2002, 2012 and 2022 ranged from - 0.641797 to 0.390728, -0.727273 to 0.441176 and -0.402645 to 0.49178 respectively (Figure 15, Figure 16 & Figure 17). There are notable changes in NDBI value during the study period. The built-up and barren rock areal coverage have increased in 2022 compared to 2002.

A declining populations trend was evident in Nepal's hill and mountain regions according to the most recent census, and 32 of the country's 77 districts resulted in negative population growth as a result of the ongoing migration of Nepali villagers to the urban area (CBS, 2021). Because of geographic variations in labor demand, diversity in resource allocation and distribution, fertile land,and easy access, the cities near the foothills of the Terai displayed expanded built-up areas (Gartaula and Niehof, 2013). In particular, after the liberalization policy in 1990 that permits unrestricted trade between the two countries, cities located close to the Indo-Nepal border experienced tremendous growth as more people moved there.

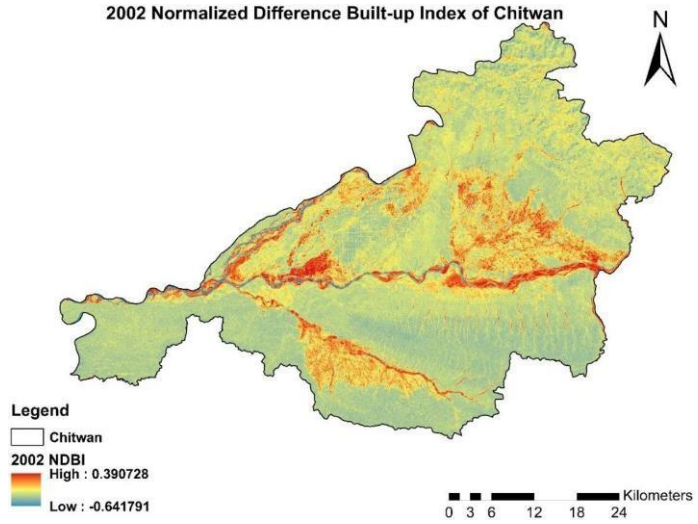

Figure 15: NDBI map of year 2002 of Chitwan District

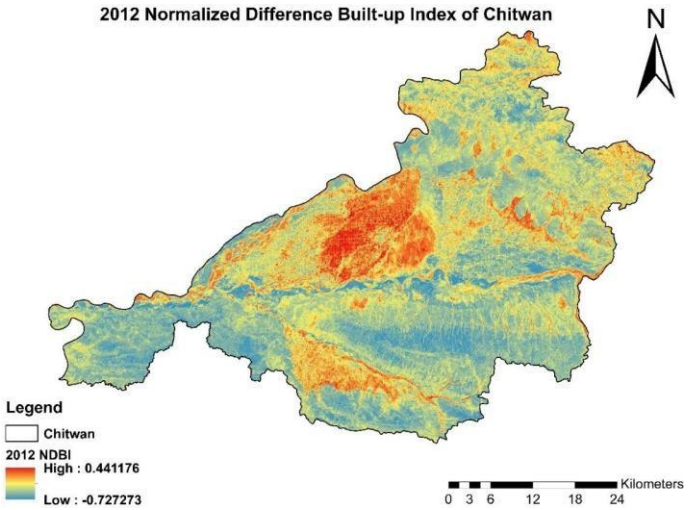

Figure 16: NDBI map of year 2012 of Chitwan District

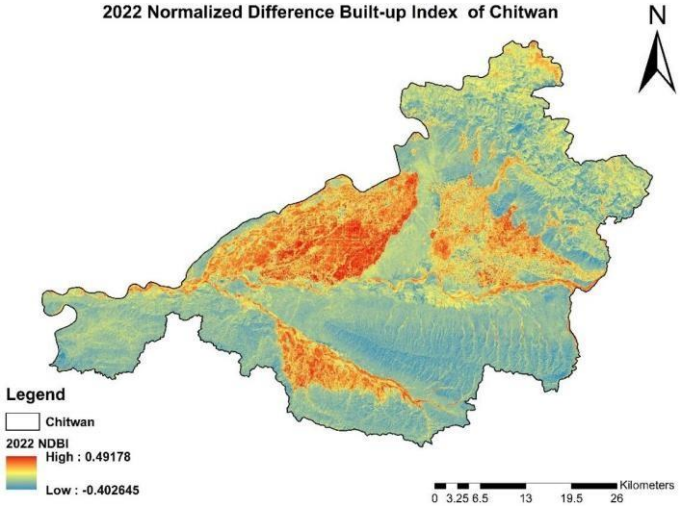

Figure 17: NDBI map of year 2022 of Chitwan District

4.4 Land surface temperature changes

In terms of LST, the changes have been significant over time. Based on Landsat thermal bands in 2002, 2012, and 2022, the spatial distribution of LSTs was calculated (Figure 18, Figure 19 and Figure 20). In 2002, the highest temperature found was 35.66°C and the lowest was 12.88°C (Figure18). In 2012, maximum temperature was 38.47°C and minimum was 16.64°C (Figure 19). During 2022 the uppermost value of temperature was analyzed 40.96°C, whereas the lowermostwas 18.52°C (Figure 20).

Overall temperature increased by 5.33◦C from 2002 to 2022 and changes found a rise of 2.81◦C from 2002 to 2012 and 2.49 ◦C from 2012 to 2022. The lowest temperature in 2002 was 12.88◦C and in 2020, it was 18.52◦C. In 30 years, a drastic change in temperature occurred. The lowest value change was 35.64◦C esteeming from 12.88◦C in 2002 to 18.52◦C in 2022. From the analysis it can be concluded that the trend of LST has been gradually increasing

from 2002 to 2022 in the study area (Figure 21).

Due to increasing rate of urbanization in Chitwan District, there is high rate of increase in the number of vehicles and factories resulting air pollution on the one hand. In other hand increasing proportion of the alphas and concrete road, high buildings, less greenery in the core urbanized area of Bharatpur Metropolitan and Ratnanagar municipality. These factors directly affected to the LST of the Chitwan district. A mountainous nation like Nepal is greatly impacted by global warming, especially in highland areas, according to studies that show the LST is raising worldwide (Chaudhary and Aryal, 2009).

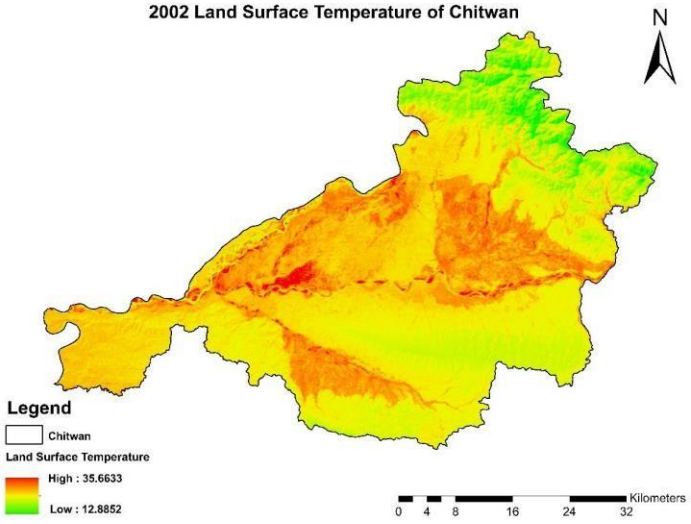

Figure 18: LST map of year 2002 of Chitwan District

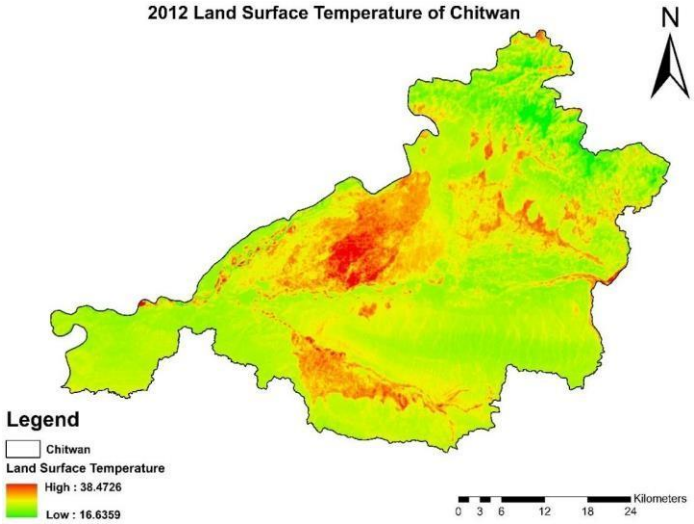

Figure 19: LST map of year 2012 of Chitwan District

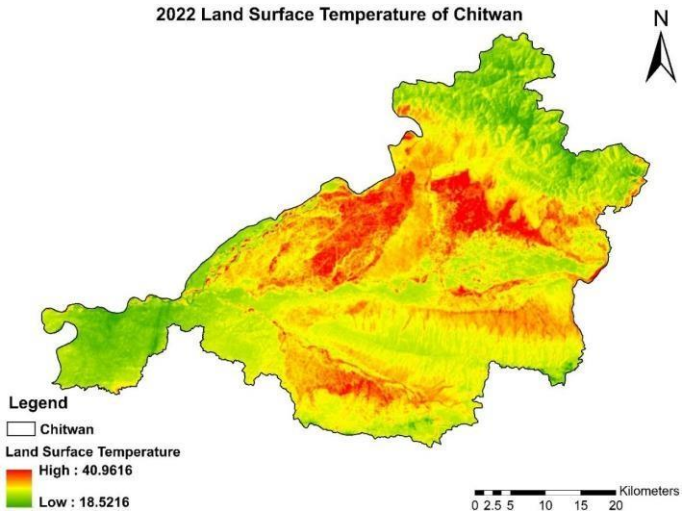

Figure 20: LST map of year 2022 of Chitwan District

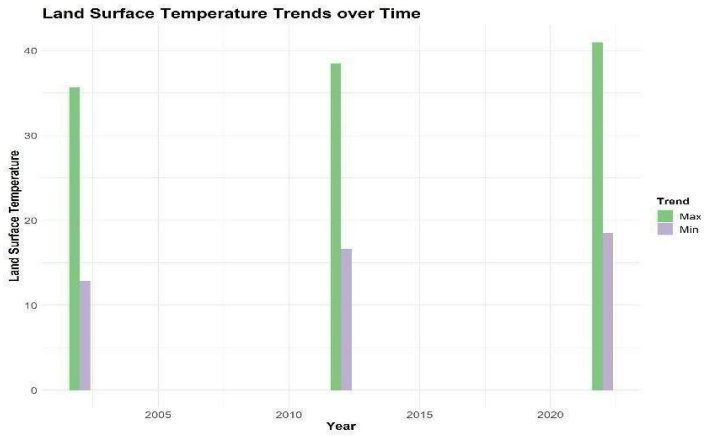

Figure 21: LST Trends over time

As a result of this study not only maximum LST is increasing but also minimum LST is increasing gradually in the study area over the time periods. In relation to LULC, the LST varies. Strong microscale patterns that are related to land categories including streets, vertical structures such as walls and roofs, trees reflectivity can be found in the LST of urban built-up areas (Roth et al., 1989). Thus, the local variability of LST of study area is highly variable due to the presence of forest, built-up area, agriculture land, water bodies and other land use classes. In order to raise the LST, LULC are crucial. But the LST can be impacted by a wide range of factors. These are the focus of subsequent research. From 2002to 2022, the proportion of LST is rising everywhere. The land's altitude, slopes also plays an essential part in determining the temperature of the land's surface. It was discovered that the LST of the inner city is higher than that of the surrounding city, the Chure Range, and the forest areas. In the study conducted by Magar et al., 2020 In comparison to other LULC surfaces, new built- up areas with compact settlement areas have higher LSTs than the less urbanized and neighboring areas, the city center has higher LST. With rising urbanization from 1999 to 2017, the LST has significantly increased. Although the ecological condition of the UHI effect is not currently in a severe state, the study's findings suggested that as urbanization continues to grow, the ecological situation in the Kathmandu Valley may become worse in coming days. According Khin et al. (2012),

and Kerr et al. (2004), land-cover changes and haphazarduse of natural resources are the main causes of the rise in LST in both rural and urban regions.

4.5 LST Validation

High temperature values were concentrated in the Chitwan District (Figure 22- Figure 24). The results of LST retrieval from Landsat shows a similar range in temperature during the study period. Itwas difficult to obtain a consistent average for climate measures in the study area. Based on the results of Landsat alone (Figures 18, 19 and 20), it is difficult to ascertain the rise in temperatures relating to the deforestation pattern, land cover change pattern and the development of urban areas. Thus, the MODIS platform was used as a guide to show the rising temperature trends.

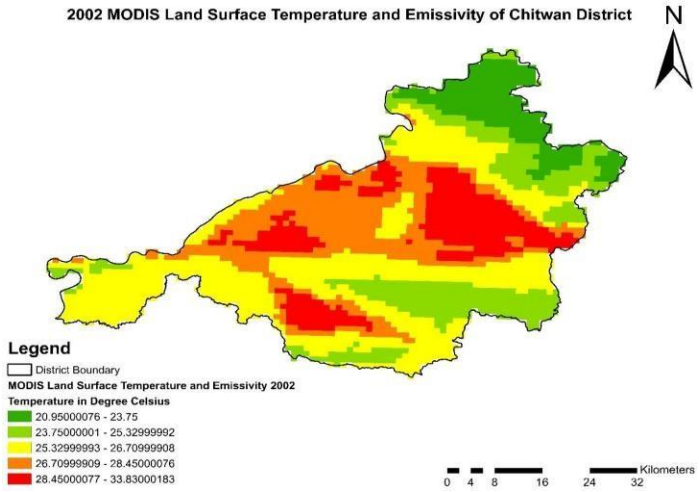

Figure 22: 2002 MODIS Land Surface Temperature and Emissivity of Chitwan

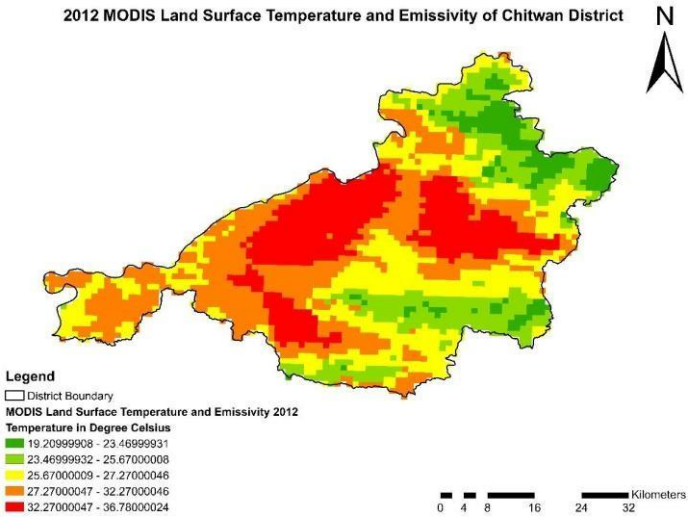

Figure 23: 2012 MODIS Land Surface Temperature and Emissivity of Chitwan

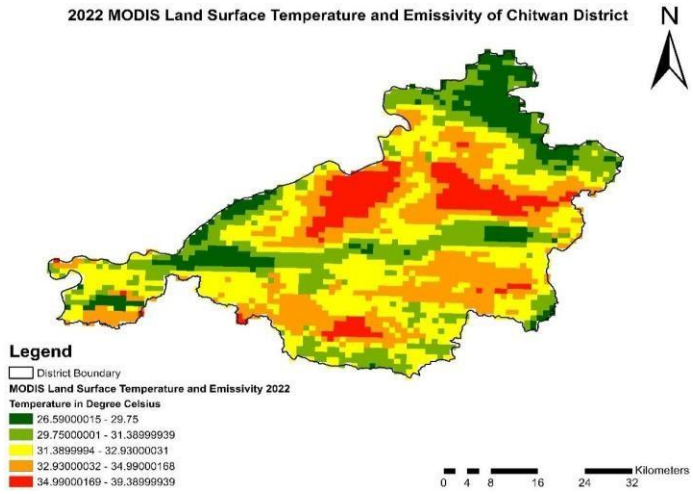

Figure 24: 2002 MODIS Land Surface Temperature and Emissivity of Chitwan

Regarding a rising temperature, the results are satisfactory, and this tendency was noticed following comparison with the different datasets. The rate of change is clearly and continuously increasing eventhough it is not as rapid as first believed. Due to clouds, as demonstrated in 2002, 2012, and 2022, Although other years provide a better picture of land surface temperature, this is a result of inadequate atmospheric correction effects. It is difficult to understand the climate throughoutthis period due to patterns and atmospheric conditions. In contrast, MODIS provides a more realistic representation of the climate in Cameron Highlands because there are no absolute highsor lows, despite the fact that monthly data variability is lower. The Landsat 8 recorded a maximum temperature of 40.96 °C in the year 2022, compared to a maximum of 39.39 °C for MODIS.In 2002 and 2012 maximum LST calculated from Landsat is 35.66 and 34.47 similarly minimum temperature is 12.89 and 16.66.While for MODIS for maximum temperature is 33.83 and 36.78and minimum temperature is 12.89 and 16.66 for 2002 and 2012 respectively. Table 9 provides an overview of the information and displays the relationship through time. Although there is a large disparity between the two sensors, the pattern of rising temperatures makes it obvious that the reported temperature is accurate.

Table 9: Comparison of LST from Landsat and MODIS validation estimation

Year	Landsat		MODIS		Landsat- MODIS	
	Max	Min	Max	Min	Max	Min
2002	35.66	12.89	33.83	20.95	1.83	-8.06
2012	38.47	16.66	36.78	19.2	1.69	-2.54
2022	40.96	18.52	39.39	26.59	1.57	-8.07

4.6 Relation between normalized indexes and LST

Variation of LST directly or indirectly depends on the LULCC and indexes. So, to investigatethe impact of land cover change on LST the relationship between LST and different land cover indices such as NDVI, NDWI and NDBI is analyzed in this research using linear regression analysis (R^2).Table 11 shows the statistics of the NDVI, NDWI, NDBI and LST in the study area ofyear 2002, 2012 and 2022.

Table 11: The statistics of the NDVI, NDWI, NDBI and LST from 2002 to 2022.

Year	NDVI		NDWI		NDBI		LST	
	Min	Max	Min	Max	Min	Max	Min	Max
2002	-0.45	0.76	-0.51	0.19	-0.64	0.39	12.89	35.66
2012	-0.12	0.57	-0.50	0.15	-0.73	0.44	16.64	38.47
2022	-0.09	0.50	-0.44	0.12	-0.40	0.49	18.52	40.96

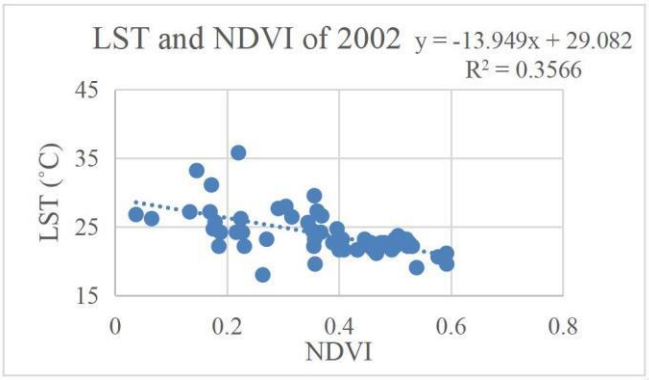

Figure 25: Relation between LST and NDVI of 2002

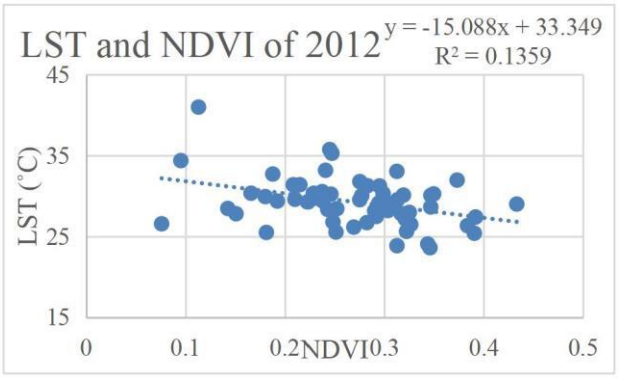

Figure 26: Relation between LST and NDVI of 2012

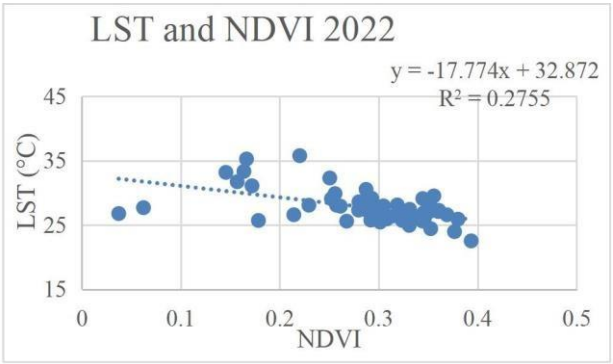

Figure 27: Relation between LST and NDVI of 2022

The spatial distribution of NDVI for year 2002, 2012 and 2022 is decrease as shown in theFigure above (Figure 9-11). The correlation between NDVI and LST for the year 2022, 2012, 2002is shown in the figure 25, figure 26 and figure 27 respectively. The regression line dramatically clarified the data, demonstrating a substantial inverse correlation between NDVI and LST. LST and NDVI are negatively associated to one another, with correlation coefficients of 0.28, 0.14, and 0.36 for the years 2022, 2012, and 2002, respectively, according to a 30-year linear regression study (R^2). These findings demonstrate that the impact of LST might lead to a reduction in

vegetationcovered regions. The lower LST is associated with increased biomass of vegetation cover, as shown by the negative association between NDVI and LST. LULC fluctuations are directly impacted by the LST and NDVI. This study found that the NDVI values have dropped between 2002 to 2022 asa result of expanding metropolitan areas and shrinking vegetated areas. Maximum LST values reveal the lowest NDVI and vice versa, and they differentiate between areas with high LST and bare soil and areas with low temperature and more vegetation.

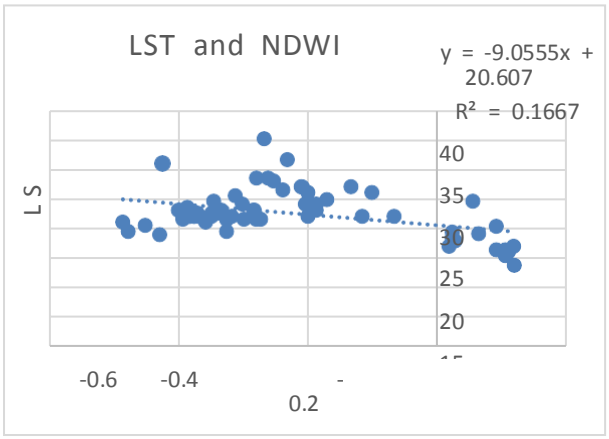

Figure 28: Relation between LST and NDWI of 2002

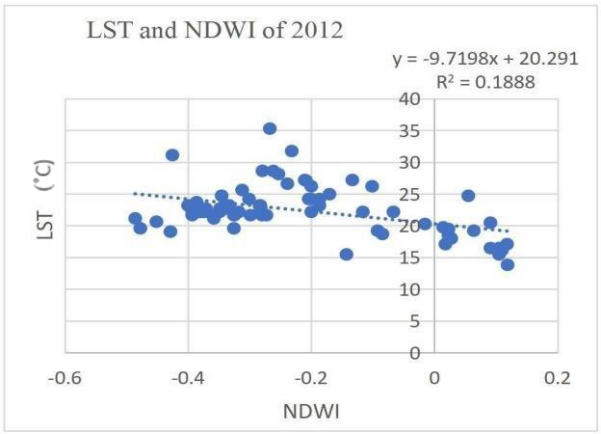

Figure 29: Relation between LST and NDWI of 2012

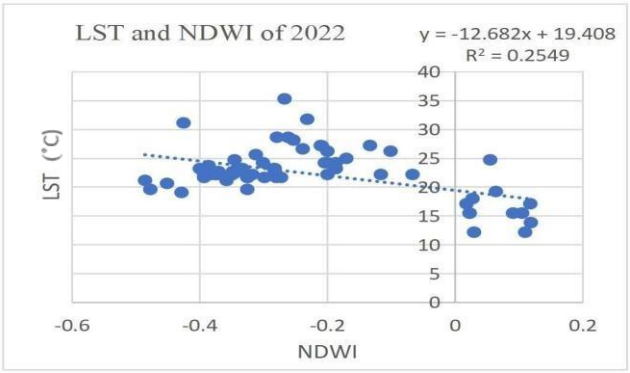

Figure 30: Relation between LST and NDWI of 2022

Figure 12, figure 13 and figure 14 shows NDWI maps in 2002, 2012 and 2022, while figure 28, figure 29 and figure 30 shows the relationship between LST and NDWI. The results of the analysisin 2002 to 2018 showed a declining trend. The present result shows a significant and negative correlation 0.25, 0.19, and 0.17 in 2022, 2012 and 2002respectively between LST and NDWI on thewater bodies throughout the period. The LST value increases as the NDWI values decrease. This demonstrates that the temperature will drop when there is more green space. From the study we cansay that NDWI is inversely proportional to LST.

Finally, regression analysis shows that LST increased with the increase of built-up area i.e NDBI and vice versa. On the other hand, LST decreased with the increased NDVI and water body indicesNDWI and vice-versa. According to Zhang et al. (2014), vegetation primarily lowers temperature through shade and evapotranspiration processes, which absorb heat energy and release water vapor.Water features can lessen the severity of UHI (Guha et al. 2018). Water bodies often have a lower temperature than other types of land usage (Zhang and Huang, 2015).

According to Rasul et al. (2017) and Chen and Zhang (2017), water bodies aid to reduce extremeheat and improve the cooling effects.

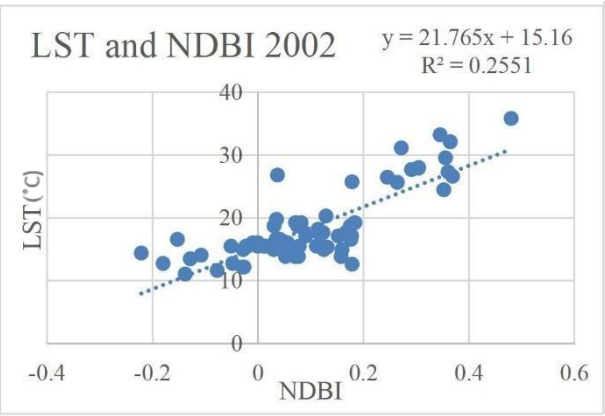

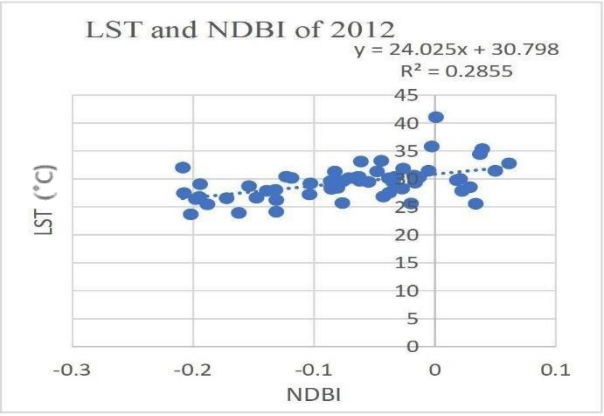

Figure 31: Relation between LST and NDBI of 2002Figure 32: Relation between LST and NDBI of 2012

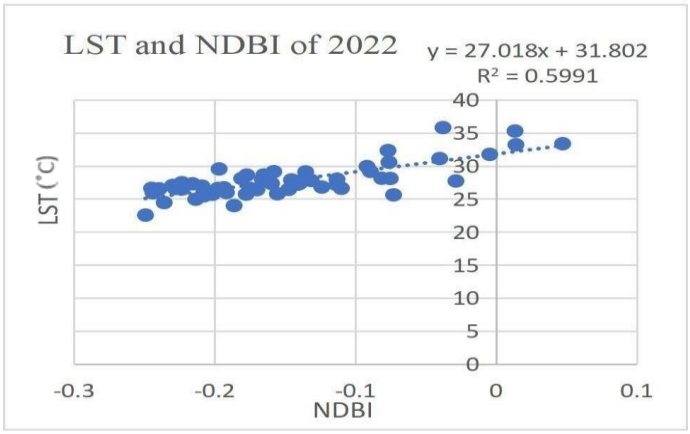

Figure 33: Relation between LST and NDBI of 2002

The research studied the association between NDBI and LST and discovered a direct relationship between them. The maximum surface temperature in built-up regions was shown by NDBI results (Figure 15 to figure 17). Therefore, it has been expected that urbanization or built-upareas willcause significant changes in LST. In NDBI & LST correlation a strong positive relationship has been existed in each season i.e. R2 = 0.26, 0.29 & 0.60 in 2022, 2012 and 2002 respectively as shown in figure 31, figure 32 and figure 33 . The observation finds that there is a positive correlation between NDBI and LST which indicates that the built-up region is the primary source of surface temperature changes and an urban heat island. LST and NDBI have a positive relationship, and NDBIindicates high LST values in the settlement and arid terrain area. The NDBI map of the present investigation is displayed above Figure 15, Figure 16 and Figure 17. According to the study's findings,built-area and barren land exhibit high LST, while forests, water bodies, cropland, shrub and grassland

habitats exhibit relatively low LST.

5.1 Main conclusions

Chapter 5 Conclusions

The immense urbanization changes brought on by Chitwan's rapidly rising population and their effects on LULC and LST change are very concerning, particularly anticipating that the populationgrowth will continue. Chitwan district have had a considerable LULC change throughout the courseof the period, with steadily growing built-up areas and declining forest areas. Spatial-temporal trends of LULC, NDVI, NDBI, NDWI, and LST and their interrelationships were systematically analyzed using Landsat 7 ETM+ and Landsat 8 OLI/TIRS remote sensing data in Chitwan of year 2002, 2012 and 2022. There was a positive relationship between LST and NDBI, and negative relation between NDVI and NDWI with LST. Over the past 20 years, built-up areas have had a very significant effect on LST compared with other LULC classes in the study area. The increase in built up areas has drastically increased the LST by 5.3°C in 2022. The findings of this study willhelp city planners formulate activities including smart city technology, urban forestry to combat the urban heat island. Furthermore, this study will provide policymakers and local governments with information on developing sustainable urban development strategies and plans to prevent haphazard urban growth, while preserving agricultural lands in the city to promote local food supply and green spaces to ensure an uninterrupted flow of ecosystem services.

5.2 Limitations of the study

As part of the present study, all possible efforts were made to gather, interpret, and analyze primaryand ancillary data. There are undoubtedly some drawbacks of utilizing Landsat imagery in Chitwanto explore the connection between LULCC and LST. As, Landsat image with a spatial resolutionof 30 meters pixel may not be able to capture the fine-scale variability of LST and LULC in study areas, especially in densely populated areas and areas with mixed cropland and densely built areas.Landsat imagery can also be partially obscured by clouds, and there are limited cloud-free photos available for study. This may result in gaps in the LULCC and LST time-series, which can make itdifficult to identify and understand long-term patterns. There may be considerable ambiguity in the computed LST and LULCC values because the Landsat sensors have undergone numerous calibration operations over the years. The accuracy of LST observations can also be impacted by changes in meteorological pressure, such as aerosol deposition, water vapor and presence of other

gases and dust particles. Landsat imagery's data availability might be constrained, especially for particular periods or locations of interest. Long- term assessments of LULCC and LST trends may find this to be a substantial restriction. It can be difficult to evaluate LULCC and LST changes using Landsat imagery, especially in areas with a variety of land use or land cover types. Moreover,elements including the complexity of the terrain, spectral confusion, as well as the reliability of thereference points might have an impact on the classifying and interpretation's accuracy. There mightbe Absence of real-world data, especially for LST, can pose a major drawback. To assure the validityof LST data, remote sensing-derived LST must be validated with ground-based observations, however this might be difficult to accomplish in inaccessible or remote locations.

Reference

Abid, S. K., Sulaiman, N., Mahmud, N. P. N., Nazir, U., & Adnan, N. A. (2022). A review on the application of remote sensing and geographic information system in flood crisis management. In *Conference on Broad Exposure to Science and Technology.—2022*.

Abid, S. K., Sulaiman, N., Chan, S. W., Nazir, U., Abid, M., Han, H., ... & Vega-Muñoz, A. (2021). Towardan integrated disaster management approach: how artificial intelligence can boost disaster management. *Sustainability*, *13*(22), 12560.

Acharyya, N., & Bandyopadhyay, J. (2017). Remote sensing and GIS for wildlife management. In National LevelSeminar on Defaunation and Conservation; Tucson Herpetological Society: Tuscon, AZ, USA (pp. 65- 71).

Adeyeri O.E and E.C. Okogbue (2014). Effect of landuse landcover on Land surface temperature. In Proceedings of Climate Change, and Sustainable Economic Development. Pp. 175-184. ISBN 978-978-521- 43-6-9

Adeyemi, A. A., & Olowo, G. E. (2022). Evaluation of forest-cover dynamics and its drivers in Okeluse Forest Reserve, Ondo State, Nigeria. *Journal of Agriculture and Environment*, *18*(1), 107-125

Agergaard, J. (1999). Settlement and changing land use in the Chitwan District of Nepal. *Geografisk Tidsskrift*, 11-20.

Aredehey G, Mezgebu A, Girma A (2018) Land-use land-cover classification analysis of Giba catchment using hyper temporal MODIS NDVI satellite images. International Journal of Remote Sensing 39(3):810–821 DOI: 10.1080/01431161.2017.1392639

Aryal, A., Shakya, B. M., Maharjan, M., Talchabhadel, R., & Thapa, B. R. (2021). Evaluation of the land surface temperature using satellite images in kathmandu valley. *Nepal Journal of Civil Engineering*, *1*(1), 1-10. https://doi.org/10.3126/njce.v1i1.43368

Bajracharya, B., Thapa, R. B., & Matin, M. A. (2021). *Earth Observation Science and Applications for Risk Reduction and Enhanced Resilience in Hindu Kush Himalaya Region: A Decade of Experience from SERVIR*(p. 375). Springer Nature.

Batar, A. K., Watanabe, T., & Kumar, A. (2017). Assessment of land-use/land-cover change and forest fragmentation in the Garhwal Himalayan Region of India. *Environments*, *4*(2), 34.

Baidya, N. G., Bhuju, D. R., & Kandel, P. (2009). Land use change in buffer zone of chitwan national park, Nepal between 1978 and 1999. *Ecoprint: An International Journal of Ecology*, *16*, 79-86.

Butt, B. (2018). Environmental indicators and governance. *Current Opinion in Environmental Sustainability*,*32*,84-89. https://doi.org/10.1016/j.cosust.2018.05.006

Cai, Z., Liu, Q., & Cao, S. (2020). Real estate supports rapid development of China's urbanization. *Land usepolicy*, *95*, 104582.

Carlson, T. N., & Sanchez-Azofeifa, G. A. (1999). Satellite remote sensing of land use changes in and around SanJose, Costa Rica. *Remote Sensing of Environment*, *70*(3), 247-256. https://doi.org/10.1016/S0034- 4257(99)00018-8

Chakraborty, K., Sivasankar, T., Lone, J. M., Sarma, K. K., & Raju, P. L. N. (2020). Status and opportunitiesfor forest resources management using geospatial technologies in northeast India. In *Spatial Information Science for Natural Resource Management* (pp. 206-224). IGI Global.

Chaudhary, P. and Aryal, K. (2009). Global warming in Nepal: Challenges and policy imperatives. *Journal of Forest and Livelihood*, 8 (1): 4-14.

Chen, J., Theller, L., Gitau, M. W., Engel, B. A., & Harbor, J. M. (2017). Urbanization impacts on surface runoff of the contiguous United States. *Journal of environmental management*, *187*, 470-481. https://doi.org/10.1016/j.jenvman.2016.11. 017

Choudhury D, Das K, Das A (2019) The Egyptian journal of remote sensing and space sciences assessment of landuse land cover changes and its impact on variations of land surface temperature in Asansol-Durgapur developmentregion. *Egypt J Remote Sens Space Sci* 22(2):203–218. https://doi.org/10.1016/j.ejrs.2018.05. 004

Collins, R., & Jenkins, A. (1996). The impact of agricultural land use on stream chemistry in the middle hillsof the Himalayas, Nepal. *Journal of Hydrology*, *185*(1-4), 71-86. https://doi.org/10.1016/0022-1694(95)03008-5

Cong, R.-G., & Brady, M. (2012). The Interdependence between Rainfall and Temperature: Copula Analyses.

The Scientific World Journal, 2012, 1–11. doi:10.1100/2012/405675

Dai, X., Johnson, B. A., Luo, P., Yang, K., Dong, L., Wang, Q., ... & Yao, Y. (2021). Estimation of urban ecosystem services value: A case study of Chengdu, Southwestern China. *Remote Sensing*, *13*(2), 207.

Dutrieux, L. P., Verbesselt, J., Kooistra, L., & Herold, M. (2015). Monitoring forest cover loss using multiple datastreams, a case study of a tropical dry forest in Bolivia. *ISPRS Journal of Photogrammetry and Remote Sensing*, *107*, 112-125

https://doi.org/10.1016/j.isprsjprs.2015.03.015

Eniolorunda, N. B., Mashi, S. A., & Nsofor, G. N. (2017). Toward achieving a sustainable management: characterization of land use/land cover in Sokoto Rima floodplain, Nigeria. *Environment, Development and Sustainability*, *19*, 1855-1878.

Eswar, R., Sekhar, M., & Bhattacharya, B. K. (2016). Disaggregation of LST over India: comparative analysisof different vegetation indices. *International Journal of Remote Sensing*, *37*(5), 1035-1054. https://doi.org/10.1080/01431161.2016.1145363

Fischlin, A., Midgley, G. F., Price, J. T., Leemans, R., Gopal, B., Turley, C., et al. (2007). "Ecosystems, their properties, goods, and services. Climate change 2007: impacts, adaptation and vulnerability," in *Proceedings of the Contribution of Working Group II to the Fourth Assessment Report of the Intergovernmental Panel on Climate Change*, eds M. L. Parry, O. F. Canziani, J. P. Palutikof, and C. E. Hanson (Cambridge: Cambridge University Press), 211–272.

Foody, G. M. (2002). Status of land cover classification accuracy assessment. *Remote sensing of environment*,*80*(1), 185-201.

Gartaula, H. N., & Niehof, A. (2013). Migration to and from the terai: shifting movements and motives. *TheSouth Asianist*, *2*(2), 28-50.

Gao, B. C. (1996). NDWI—A normalized difference water index for remote sensing of vegetation liquid waterfrom space. *Remote sensing of environment*, *58*(3), 257-266.

Geremeskel, T., & Abera, M. (2017). The need for transformation: Local perception of climate change, vulnerability and adaptation versus 'Humanitarian'response in Afar Region, Ethiopia. *Climate Change Adaptationin Africa: Fostering Resilience and Capacity to Adapt*, 511-529.

Ghimire, R., Dhakal, S., Sapkota, M., Yogesh, K. C., & Shrestha, R. (2022). Web Mapping on Land Cover Changeof Kathmandu, Lalitpur and Bhaktapur District. *Journal on Geoinformatics, Nepal*. https://doi.org/10.3126/njg.v21i1.50887

Guha, S., Govil, H., Dey, A., & Gill, N. (2018). Analytical study of land surface temperature with NDVI and NDBIusing Landsat 8 OLI and TIRS data in Florence and Naples city, Italy. European *Journal of Remote Sensing*, 51(1),667-678. https://doi.org/10.1080/22797254.2018.1474494.

Govind, N. R., & Ramesh, H. (2019). The impact of spatiotemporal patterns of land use land cover and land surface temperature on an urban cool island: a case study of Bengaluru. *Environmental monitoring and assessment*, *191*, 1-20.

Goldstein, M. I., & DellaSala, (2020). *Encyclopedia of the World's Biomes*. Elsevier.

Haregeweyn, N., Tesfaye, S., Tsunekawa, A., Tsubo, M., Meshesha, D. T., Adgo, E., & Elias, A. (2015). Dynamicsof land use and land cover and its effects on hydrologic responses: case study of the Gilgel Tekeze catchment in the highlands of Northern Ethiopia. *Environmental monitoring and assessment*, *187*, 1-14.

Helmer, E. H., Brown, S., & Cohen, W. B. (2000). Mapping montane tropical forest successional stage and land use with multi-date Landsat imagery. *International journal of remote sensing*, *21*(11), 2163-2183

Hoelscher, K., & Aijaz, R. (2016). Challenges and opportunities in an urbanising India. *International Area StudiesReview*, *19*(1), 3-11. https://doi.org/10.1177/2233865916637297

Hooker, J., Duveiller, G., & Cescatti, A. (2018). A global dataset of air temperature derived from satellite remote sensing and weather stations. Scientific data, 5(1), 1-11.

Hua, A. K., and Ping, O. W. (2018). The influence of land-use/land-cover changes on land surface temperature: a case study of Kuala Lumpur metropolitan city. *Eur. J. Remote Sens.* 51, 1049–1069. doi: 10.1080/22797254.2018.1542976

Huang, Y., Raza, S. M. F., Hanif, I., Alharthi, M., Abbas, Q., and Zain-ul-Abidin, S. (2020). The role of forest resources, mineral resources, and oil extraction in economic progress of developing Asian economies. *Resour. Policy* 69, 101878. doi: 10.1016/j.resourpol.2020.101878

Hulley, G. C., Ghent, D., Göttsche, F. M., Guillevic, P. C., Mildrexler, D. J., & Coll, C. (2019). Land surface temperature. In *Taking the Temperature of the Earth* (pp. 57-127). Elsevier. https://doi.org/10.1016/B978-0- 12-814458-9.00003-4

Hussain, A., Madan, R., & Kamboj, V. (2022). Applications of remote sensing and GIS in hydrological and hydrogeological studies: integrated watershed management. In *Addressing Environmental Challenges Through Spatial Planning* (pp. 237-251). IGI Global.

Jayanth, J., Koliwad, S. and Kumar, T. 2015. Classification of Remote Sensed Data Using Artificial Bee Colony Algorithm. *The Egyptian Journal of Remote Sensing and Space Science*, 18(1): 119-126.

Jiang, Y., & Lin, W. (2021). A comparative analysis of retrieval algorithms of land surface temperature from Landsat-8 data: a case study of Shanghai, China. International Journal of Environmental Research and Public Health, 18(11), 5659.

James, M., & Charles, N. .2014. Spatial-temporal effects of land use changes on land surface temperature in Nairobi. In Proceedings of sustainable research and innovation conference .pp. 26–29.

Jones, H. G., & Vaughan, R. A. (2010). *Remote sensing of vegetation: principles, techniques, and applications*. Oxford university press.

Kerr, Y.H., Lagouarde, J.P., Nerry, F., Ottle, C. (2004). Land surface retrieval techniques and applications: case of AVHRR, in: Quatrocci, D.A., Luvall, J. C. *Thermal remote sensing in land surface processes*. CRC press,Florida, USA, 33–109.

Khin, M.Y., Shin D.Y., Park, J.J., Choi C.C., (2012). Land surface temperature changes by LU changes of Inlay Lake area, Myanmar. Department of Spatial Information Engineering, Pukyong National University, South Korea.

Lawrence, P. J., & Chase, T. N. .(2007). Representing a new MODIS consistent land surface in the Community Land Model .CLM 3.0. Journal of Geophysical Research: Biogeosciences, 112.G1.

Lele, N., & Joshi, P. K. (2009). Analyzing deforestation rates, spatial forest cover changes and identifying criticalareas of forest cover changes in North-East India during 1972–1999. *Environmental monitoring and assessment*, *156*, 159-170.

Lillesand, T., Kiefer, R. W., & Chipman, J. (2015). *Remote sensing and image interpretation*. John Wiley & Sons.

Liu, P., Jia, S., Han, R., Liu, Y., Lu, X., & Zhang, H. (2020). RS and GIS supported urban LULC and UHI changesimulation and assessment. *Journal of Sensors*, *2020*, 1-17. https://doi.org/10.1155/2020/5863164

Liu J, Xiao W, Jiang Z, Feng X, Li X (2005) A study on the influence of landscape fragmentation on biodiversity.For Res 18(2):222–226

Liu, Y., Peng, J., & Wang, Y. (2018). Efficiency of landscape metrics characterizing urban land surface temperature. *Landscape and Urban Planning*, *180*, 36-53.

Lu, D., Mausel, P., Brondizio, E. & Moran, E. (2004). Change detection techniques. International Journal of Remote Sensing, 25(12), pp.2365-2401.

Magar, D. S., Magar, R. K. S., & Chidi, C. L. (2021). Assessment of urban heat island in Kathmandu valley (1999-2017). *Geographical Journal of Nepal*, *14*, 1-20.Maktav, D., Erbek, F. S., & Jürgens, C. (2005). Remote sensing of urban areas. *International journal of remote sensing*, *26*(4), 655-659.

https://doi.org/10.1080/01431160512331316469

Ma, Y. (2004). GIS application in watershed management. *Nature and Science*, *2*(2), 1-7.

Manfré, L. A., Hirata, E., Silva, J. B., Shinohara, E. J., Giannotti, M. A., Larocca, A. P. C., & Quintanilha, J. A. (2012). An analysis of geospatial technologies for risk and natural disaster management. *ISPRS International Journal of Geo-Information*, *1*(2), 166-185.

Mani, J. K., & Varghese, A. O. (2018). Remote sensing and GIS in agriculture and forest resource monitoring.

Geospatial technologies in land resources mapping, monitoring and management, 377-400.

Maus, V., Giljum, S., da Silva, D. M., Gutschlhofer, J., da Rosa, R. P., Luckeneder, S., ... & McCallum, I. (2022).

An update on global mining land use. *Scientific data*, *9*(1), 433. https://doi.org/10.1038/s41597-022- 01547-4

McFeeters, S. K. (1996). The use of the Normalized Difference Water Index (NDWI) in the delineation of open water features. *International journal of remote sensing*, *17*(7), 1425-1432.

Meshesha, D. T., Tsunekawa, A., Tsubo, M., Ali, S. A., & Haregeweyn, N. (2013). Land-use change and its socio-environmental impact in Eastern Ethiopia's highland. *Regional Environmental Change, 14(2), 757–768*. doi:10.1007/s10113-013-0535-2

Meyer, W. B., & BL Turner, I. I. (Eds.). (1994). *Changes in land use and land cover: a global perspective*

(Vol. 4). Cambridge University Press.

Meyfroidt, P., Chowdhury, R. R., de Bremond, A., Ellis, E. C., Erb, K. H., Filatova, T., ... & Verburg, P. H. (2018).

Middle-range theories of land system change. *Global environmental change*, *53*, 52-67. https://doi.org/10.1016/j.gloenvcha.2018.08.0

Myers-Smith, I. H., Forbes, B. C., Wilmking, M., Hallinger, M., Lantz, T., Blok, D., ... & Hik, D. S. (2011). Shrubexpansion in tundra ecosystems: dynamics, impacts and research priorities. *Environmental Research Letters*, *6*(4),045509.

Ogunjobi, K. O., Adamu, Y., Akinsanola, A. A., & Orimoloye, I. R. (2018). Spatio-temporal analysis of landuse dynamics

and its potential indications on land surface temperature in Sokoto Metropolis, Nigeria. *Royal Societyopen science*, *5*(12), 180661.

Ojima, D. S., Galvin, K. A., & Turner, B. L. (1994). The global impact of land-use change. BioScience, 44(5), 300

Ouyang, W., Skidmore, A. K., Toxopeus, A. G., & Hao, F. (2010). Long-term vegetation landscape pattern with non-point source nutrient pollution in upper stream of Yellow River basin. *Journal of Hydrology*, *389*(3- 4), 373-380.

Pal, S., and Ziaul, S. (2017). Detection of land use and land cover change and land surface temperature in EnglishBazar urban centre. *Egypt J. Remote Sens. Space Sci.* 20, 125–145

Pal, M., & Mather, P. M. J. R. soe (2003). *An assessment of the effectiveness of decision tree methods for land cover classification*, *86*(4), 554-565.

Pande, C. B., & Pande, C. B. (2020). Watershed management and development. *Sustainable Watershed Development: A Case Study of Semi-arid Region in Maharashtra State of India*, 13-26.

Peng, X., Wu, W., Zheng, Y., Sun, J., Hu, T., & Wang, P. (2020). Correlation analysis of land surface temperatureand topographic elements in Hangzhou, China. *Scientific Reports*, *10*(1), 10451.

Panta, M., Kim, K., & Joshi, C. (2008). Temporal mapping of deforestation and forest degradation in Nepal: Applications to forest conservation. *Forest Ecology and Management*, *256*(9), 1587-1595.

Paudel, B., Zhang, Y. L., Li, S. C., Liu, L. S., Wu, X., & Khanal, N. R. (2016). Review of studies on land use and land cover change in Nepal. *Journal of Mountain Science*, *13*, 643-660.

Pettorelli, N., Vik, J. O., Mysterud, A., Gaillard, J. M., Tucker, C. J., & Stenseth, N. C. (2005). Using the satellite-derived NDVI to assess ecological responses to environmental change. *Trends in ecology & evolution*, *20*(9), 503-510.

Policelli, F., Hubbard, A., Jung, H. C., Zaitchik, B., & Ichoku, C. (2018). Lake Chad total surface water area as derived from land surface temperature and radar remote sensing data. *Remote Sensing*, *10*(2), 252. https://doi.org/10.3390/rs10020252

Pontius, R. G. (2002). Statistical methods to partition effects of quantity and location during comparison of categorical maps at multiple resolutions. *Photogrammetric engineering and remote sensing*, *68*(10), 1041.

Rahman, M. S., Mohiuddin, H., Kafy, A. A., Sheel, P. K., & Di, L. (2019). Classification of cities in Bangladesh based on remote sensing derived spatial characteristics. *Journal of Urban Management*, *8*(2), 206- 224.

Rai, R., Yili, Z., Paudel, B., Khanal, N. R., & Acharya, B. K. (2020). Satellite image-based monitoring of urban land use change and assessing the driving factors in Pokhara and Bharatpur metropolitan cities, Gandaki Basin, Nepal. *Journal of resources and ecology*, *11*(1), 87-99. https://doi.org/10.5814/j.issn.1674- 764x.2020.01.009

Ramasubramanian, L. (2009). Book Review: Wade, T., and S. Sommer, eds. 2006. A to Z GIS: An illustrated dictionary of geographic information systems. Redlands, CA: ESRI Press. 288 pp. $24.95 paperback, ISBN 1- 5894-8140-2. *Journal of Planning Literature*, *23*(3), 263-264.

Rees, W., & Wackernagel, M. (2008). Urban ecological footprints: why cities cannot be sustainable—and why they are a key to sustainability. *Urban ecology: an international perspective on the interaction between humans and nature*, 537-555.

Rimal, B., Sloan, S., Keshtkar, H., Sharma, R., Rijal, S., & Shrestha, U. B. (2020). Patterns of historical and futureurban expansion in Nepal. *Remote Sensing*, *12*(4), 628. https://doi.org/10.3390/rs12040628

Rokaya, M. B., Münzbergová, Z., Shrestha, M. R., & Timsina, B. (2012). Distribution patterns of medicinal plantsalong an elevational gradient in central Himalaya, Nepal. *Journal of Mountain Science*, *9*, 201-213. https://doi.org/10.1007/s11629-012-2144-9

Roth, M., Oke, T. R., & Emery, W. J. (1989).Satellite-derived urban heat island from three coastal cities andthe utilization of such data in urban climatology. *International Journal of Remote Sensing*, 10: 1699–1720

Roy, P. S., Dutt, C. B. S., & Joshi, P. K. (2002). Tropical forest resource assessment and monitoring. *Tropical Ecology*, *43*(1), 21-37.

Rasul, A., Balzter, H., Smith, C., Remedios, J., Adamu, B., Sobrino, J. A,. & Weng, Q. (2017). A review on remotesensing of urban heat and cool islands. Land, 6(2), 38. https://doi. org/10.3390/land6020038

Russell, G., and K. G. Congalton. (2013). Assessing the Accuracy of Remotely Sensed Data. Vol. 53. ISBN 9788578110796

Sharma, R., Ghosh, A., & Joshi, P. K. (2013). Spatio-temporal footprints of urbanisation in Surat, the Diamond City of India (1990–2009). *Environmental monitoring and assessment*, *185*, 3313-3325. https://doi.org/10.1007/s10661-012-2792-9

Singh, D., Sao, R., & Singh, K. P. (2007). A remote sensing assessment of pest infestation on sorghum.

Advances in Space Research, *39*(1), 155-163. https://doi.org/10.1016/j.asr.2006.02.025

Smart, D. R., Whiting, M. L., & Stockert, C. (2007). Remote sensing of grape K deficiency symptoms usingleaf level hyperspectral reflectance. In *Western Nutrient Management Conference* (Vol. 7, pp. 19-24).

Solanky, V., Singh, S., & Katiyar, S. K. (2018). Land surface temperature estimation using remote sensingdata. In Hydrologic Modeling: Select Proceedings of ICWEES-2016 (pp. 343-351). Springer Singapore.

Stapp, J. R., Lilieholm, R. J., Upadhaya, S., & Johnson, T. (2015). Evaluating the impacts of forest management policies and community-level institutions in the buffer zone of Chitwan National Park, Nepal. *Journalof Sustainable Forestry*, *34*(5), 445-464.

Timilsina, R. H., Ojha, G. P., Nepali, P. B., & Tiwari, U. (2019). Agriculture land use in Nepal: prospects and impacts on food security. *Journal of Agriculture and Forestry University*, *3*, 1-9.

Tomlinson, C. J., Chapman, L., Thornes, J. E., & Baker, C. (2011). Remote sensing land surface temperaturefor meteorology and climatology: A review. *Meteorological Applications*, *18*(3), 296-306. https://doi.org/10.1002/met.287

Tran, D. X., Pla, F., Latorre-Carmona, P., Myint, S. W., Caetano, M., & Kieu, H. V. (2017). Characterizing the relationship between land use land cover change and land surface temperature. *ISPRS Journal of Photogrammetryand Remote Sensing*, *124*, 119-132. https://doi.org/10.1016/j.isprsjprs.2017.01.001

Twumasi, N. Y. D., Shao, Z., & Orhan, A. (2019). Remote sensing and gis methods in urban disaster monitoring and management–an overview. *Int. J. Trend Sci. Res. Dev*, *3*, 918-926.

Van Westen, C. J. (2000). Remote sensing for natural disaster management. *International archives of photogrammetry and remote sensing*, *33*(B7/4; PART 7), 1609-1617.

Varghese, A. O., Mani, J. K., & Jha, C. S. (2022). Applications of Geospatial Technology in Forest Resource Assessment, Management, and Monitoring. In *Geospatial Technologies for Resources Planning and Management*(pp. 663-690). Cham: Springer International Publishing.

Verburg, P. H., Neumann, K. & Nol, L. 2011. Challenges in using land use and land cover data for global change studies. Global Change Biology, 17(2), pp.974-989.

Verma, R. K., Kumari, S., & Tiwary, R. K. (2009). Application of remote sensing and GIS technique for efficienturban planning in India. In *Geomatrix conference proceedings*.

Verma, P., Raghubanshi, A., Srivastava, P. K., and Raghubanshi, A. S. (2020). Appraisal of kappa-basedmetrics and disagreement indices of accuracy assessment for parametric and nonparametric techniques used in LULC classification and change detection. *Model. Earth Syst. Environ.* 6, 1045–1059.

Vicente-Serrano, S. M., Camarero, J. J., Olano, J. M., Martín-Hernández, N., Peña-Gallardo, M., Tomás- Burguera,M., ... & El Kenawy, A. (2016). Diverse relationships between forest growth and the Normalized Difference Vegetation Index at a global scale. *Remote Sensing of Environment*, *187*, 14-29. https://doi.org/10.1016/j.rse.2016.10.001

Vlassova, L., & Pe´rez-Cabello, F..2016. Effects of post-fire wood management strategies on vegetation recoveryand land surface temperature. LST estimated from Landsat images. International Journal of Applied Earth Observation and Geoinformation, 44, 171–183.

Wan, Z., Zhang, Y., Zhang, Q., & Li, Z. L. (2004). Quality assessment and validation of the MODIS global land surface temperature. *International journal of remote sensing*, *25*(1), 261-274.

Wang, S. W., Gebru, B. M., Lamchin, M., Kayastha, R. B., & Lee, W. K. (2020). Land use and land cover changedetection and prediction in the Kathmandu district of Nepal using remote sensing and GIS. *Sustainability*, *12*(9), 3925. https://doi.org/10.3390/su12093925

Wardlow, B. D., Anderson, M. C., & Verdin, J. P. (Eds.). (2012). *Remote sensing of drought: Innovative monitoringapproaches*. CRC Press.

Wilkie, D. S., Finn, J. T., & Finn, J. (1996). *Remote sensing imagery for natural resources monitoring: a guide forfirst-time users*. Columbia University Press.

Wei, M. A., Yun-hao, C., & Ji, Z. .(2008). Quantitative analysis of land surface temperature vegetation indexes relationship based on remote sensing. The International Archives of the Photogrammetry, Remote Sensing and Spatial Information Sciences, XXXVII..Part31 B6b, 261–264.

Winkler, K., Fuchs, R., Rounsevell, M., & Herold, M. (2021). Global land use changes are four times greater thanpreviously estimated. *Nature communications*, *12*(1), 2501.

Wu, C., Niu, Z., Tang, Q., & Huang, W. (2009). Predicting vegetation water content in wheat using normalized difference water indices derived from ground measurements. *Journal of plant research*, *122*, 317- 326.

Wu, H., Hao, Y., & Weng, J. H. (2019). How does energy consumption affect China's urbanization? New evidencefrom dynamic threshold panel models. *Energy policy*, *127*, 24-38.

Wu, Q., Li, H. Q., Wang, R. S., Paulussen, J., He, Y., Wang, M., ... & Wang, Z. (2006). Monitoring and predicting land use change in Beijing using remote sensing and GIS. *Landscape and urban planning*, *78*(4), 322-333. https://doi.org/10.1016/j.landurbplan.2005.10.0
02

World Wildlife Fund for Nature (WWF). (2013). Chitwan annapurna landscape (CHAL): a rapid assessment. *World Wildlife Fund Nepal: Kathmandu, Nepal*.

Xiaomei, Y., & RongQing, L. Q. Y. (1999). Change Detection Based on Remote Sensing Information Modeland its Application on Coastal Line of Yellow River Delta. *Earth Observation Center, NASDA, China*.

Yan, Y., Mao, K., Shi, J., Piao, S., Shen, X., Dozier, J., ... & Bao, Q. (2020). Driving forces of land surfacetemperature anomalous changes in North America in 2002–2018. *Scientific reports*, *10*(1), 6931.

Yang, Y., Lin, H., Guo, Z., & Jiang, J. (2007). A data mining approach for heavy rainfall forecasting based on satellite image sequence analysis. *Computers & geosciences*, *33*(1), 20-30.
https://doi.org/10.1016/j.cageo.2006.05.010

Yang, X., Zheng, X. Q., & Chen, R. (2014). A land use change model: Integrating landscape pattern indexes and Markov-CA. *Ecological Modelling*, *283*, 1-7.

Yuan, Z., Xu, J., Wang, Y., & Yan, B. (2021). Analyzing the influence of land use/land cover change on landscapepattern and ecosystem services in the Poyang Lake Region, China. *Environmental Science and Pollution Research*,*28*, 27193-27206.

Yue, W., Xu, J., Tan, W., & Xu, L (2007). The relationship between land surface temperature and NDVI with remote sensing: Application to Shanghai Landsat 7 ETM + data. International Journal of Remote Sensing, 28.15,3205–3226.

Zhang, W., & Huang, B. (2015). Land use optimization for a rapidly urbanizing city with regard to local climate change: Shenzhen as a case study. *Journal of Urban Planning and Development*, 141(1), 05014007. doi:10.1061/ (ASCE)UP.1943-5444.0000200.

Zhao, D., Reddy, K. R., Kakani, V. G., & Reddy, V. R. (2005). Nitrogen deficiency effects on plant growth, leaf photosynthesis, and hyperspectral reflectance properties of sorghum. *European journal of agronomy*, *22*(4), 391-403.

Zhao, F., Li, H., Li, C., Cai, Y., Wang, X., & Liu, Q. (2019). Analyzing the influence of landscape pattern changeon ecological water requirements in an arid/semiarid region of China. *Journal of hydrology*, *578*, 124098.

Zhou, Y., Varquez, A. C., & Kanda, M. (2019). High-resolution global urban growth projection based on multipleapplications of the SLEUTH urban growth model. *Scientific data*, *6*(1), 34.
https://doi.org/10.1038/s41597-019-0048-z

Zhu, X., & Liu, D. (2015). Improving forest aboveground biomass estimation using seasonal Landsat NDVItime-series. *ISPRS Journal of Photogrammetry and Remote Sensing*, *102*, 222-231.

Zhu, Z., Liu, B., Wang, H., & Hu, M. (2021). Analysis of the spatiotemporal changes in watershed landscape pattern and its influencing factors in rapidly urbanizing areas using satellite data. *Remote Sensing*, *13*(6), 1168.